Circadian Regulation of Sleep in *Drosophila*: Insights from a Two-Process Model

Lakshman Abhilash, Orie Thomas Shafer[#]

The Advanced Science Research Center, The City University of New York; The Graduate Center at the City University of New York

Running title: Drosophila two-process model

[#]Correspondence: oshafer@gc.cuny.edu

Abstract

Sleep is largely controlled by two processes – a circadian clock that regulates its timing and a homeostat that regulates the drive to sleep. *Drosophila* has been a useful model for understanding the molecular and neuronal control of both of these processes. Consequently, mechanisms underlying both the circadian and the homeostatic regulation of sleep have been characterized in the fly. For over four decades, Borbély and Daan's two-process model has provided a powerful quantitative framework for understanding how circadian and homeostatic processes converge to regulate sleep. Despite the clear utility of this model for understanding mammalian sleep regulation, the field of fly sleep has not employed a formal two-process model as a framework for the investigation of sleep control. To this end, we have adapted the two-process model to the fly. In this study, we establish the utility of this model by showing that it can provide empirically testable predictions regarding both the circadian and homeostatic control of fly sleep. Using this model, we show that the ultradian rhythms previously reported for loss-of-function clock mutants are a predictable consequence of a functional sleep homeostat in the absence of a functioning circadian system. Though a two-process model in which the circadian and homeostatic components act without influencing one another's rates captures qualitative aspects of sleep remarkably well, we found that increasing the rates of sleep pressure changes when circadian clocks run faster produced better quantitative fits between predicted and observed sleep rhythms. Finally, our results indicate that longer sleep bouts better reflect the homeostatic process than the current unitary definition of sleep as any bout of inactivity lasting five minutes or more. This simple two-process model represents a powerful theoretical framework for future work on the molecular and physiological regulation of fly sleep.

Keywords: Drosophila, sleep, circadian, sleep homeostat, two-process model, free-running, period, ultradian rhythms

Introduction

Sleep-like states are ubiquitous within the animal kingdom [1] and the complexity of sleep behavior has prompted many attempts to mathematically model its regulation. Such models provide a powerful quantitative framework for the experimental investigation of sleep regulation across taxa. They are particularly useful by virtue of their provision of testable hypotheses [2–9].

Among the most successful models of sleep regulation are variants of Borbély's two-process model [2,4–7], which posits the presence of a sleep pressure that builds during wakefulness (Fig. 1A). Once this sleep pressure reaches an upper threshold, sleep is induced. During sleep, pressure falls until it reaches a lower threshold, at which point wakefulness is initiated. According to this model, the build-up and discharge of sleep pressure is driven by one process – the sleep homeostatic component or the S-process, whereas the upper and lower thresholds change predictably throughout the day and are set by a second process– the circadian clock or the C-process (Fig. 1A). Though myriad factors impact sleep [10], the regulation of typical sleep/wake cycles can be explained by just these two processes acting in concert but operating independently, that is, the S-process can operate without a functional C-process and *vice versa* [6,7]. Throughout this study we use the term 'independently' to mean that the speed of the circadian clock (process C) does not depend on or influence the rates of change of process S.

The two-process model has provided a powerful conceptual framework in the field for nearly four decades owing to its ability to predict the timing and amount of sleep, particularly in humans, both during normal sleep/wake cycles and in the aftermath of sleep deprivation [5–7]. The model has also been used over the years to inform sleep clinicians in the treatment of sleep disorders

associated with major depression, seasonal affective disorders, irregular sleep patterns, and the application of bright light therapy [7]. Additionally, the model provides a powerful, quantitative framework for assessing interactions between the two processes and how they might contribute to the control of sleep [11]. Despite the longstanding utility of the two-process model for understanding human sleep, it has been underutilized as a quantitative platform for understanding the regulation of sleep in model systems amenable to the genetic and molecular manipulation of the brain.

Although *Drosophila* has proved to be a critical model system for understanding the genetic, neuronal and physiological bases of circadian rhythms since the 1970s, it has become an informative model for understanding sleep only over the past two decades [12–14]. Furthermore, because of the availability of a powerful array of genetic tools and the ability to regulate gene expression spatially and temporally in the fly, the *Drosophila* sleep field has made significant advances in understanding the regulation of sleep [15–17]. While much of the focus of fly sleep research has been on the identification of genes and neural networks that regulate the amounts of sleep [14,16,18–27] relatively little is known about the regulation of sleep timing (e.g., [28]). Therefore, much remains to be learned about how circadian clocks and homeostatic control mechanisms interact to regulate sleep.

While there are significant gaps in our understanding of sleep regulation, the fly continues to provide insights into its mechanisms [14]. A major reason for this is the apparent similarity (behavioral, genetic, and physiological) between fly and mammalian sleep [29]. For example, as in mammals, flies display bouts of extended inactivity characterized by increased arousal

thresholds, rapid reversibility, and homeostatic rebound in response to sleep deprivation [12,15,30]. In addition, a major feature of mammalian sleep is the occurrence of distinct stages of sleep, i.e., rapid eye movement (REM) and several non-REM (NREM) sleep stages [31]. Although various durations of inactivity have previously been classified as distinct epochs of sleep [12,32], fly sleep is now almost universally treated as a unitary state, with any period of inactivity lasting more than five minutes being considered a sleep like state [14,32]. However, recent work has provided strong evidence for multiple sleep stages in flies, with longer bouts of inactivity representing physiologically, metabolically, and behaviorally distinct sleep states compared to shorter bouts [33–39].

Owing to the predictive power of the two-process model of human sleep regulation, we sought to establish a quantitative theoretical framework for a two-process model of fly sleep. Here we describe the adaptation of such a model, identify the sleep homeostatic parameters that best explain fly sleep, and use it to reveal interesting relationships between sleep and the circadian clock and highlight the utility of this powerful model in understanding fly sleep. Based on this work, we propose that longer durations of inactivity, which have been recognized by others as reflecting relatively deep sleep, are a likely a stronger reflection of sleep homeostatic processes in *Drosophila* than the currently employed unitary definition of fly sleep as any bout of inactivity lasting five minutes or more.

Results

Circadian time-series analysis of *Drosophila* sleep

Though sleep is considered a major output of the circadian system, sleep behavior in flies has rarely been subjected to circadian time-series analysis. The vast majority of studies use locomotor activity, typically measured as infrared beam crossings, for such analyses. However, to fully understand the circadian control of sleep, time-series analyses should be performed directly on sleep data. For this reason, we have developed an analysis package [40], which is now available on the Comprehensive R Archive Network (CRAN; https://cran.r-project.org/web/packages/phase/index.html). Like double plotted actograms for locomotor activity, sleep rhythms can be visualized as double plotted "somnograms" (Fig. 1B). Consistent with previous work [12,14,30], somnograms reveal two distinct phases of increased sleep under light/dark (LD) cycles, one during the daytime and one during the nighttime (Fig. 1B). Although the field has long recognized that fly sleep is bimodal, in that there are two major episodes of sleep in each diurnal or circadian cycle [12,14,30], traditional time-series methods to quantitatively assess bimodality and periodicity in sleep time-series have not been employed. We used the Chi-squared (χ^2) periodogram [41] on sleep time-series data to analyze the two daily peaks of sleep under both LD cycles and constant darkness (DD), revealing two clear peaks in the periodogram, one at 12-h and the other at 24-h (Fig. 1C). Though largely similar, there are subtle differences between the periodograms of sleep and activity data measured under LD cycles and DD (Figs. 1C and 1D, compare across panels and see Table 1). The powers of average sleep time-series are higher than the powers of locomotor activity time-series (see Table 1). This is not a mere consequence of using the Chi-square periodogram, whose limitations for the quantitative

assessment of rhythmic power has been described [42–44], as similar results were also obtained using the Lomb-Scargle periodogram (Suppl. Table 1).

Using the Chi-square periodogram, the 12-h peak is typically lower than the 24-h peak in periodograms, but this difference is much smaller for the locomotor activity periodograms – in other words, the 12- and 24-h periodogram peaks are of more comparable height for locomotor activity (compare Figs. 1C and 1D). Therefore, we emphasize that irrespective of the periodogram method used, it is critical to employ sleep data to perform long-term time-series analyses rather than using locomotor activity, if one is to address the circadian regulation of sleep. Using the last four cycles under entrainment, we estimated the percentage of a 24-h day that a fly spends sleeping. Across the three genotypes, we found that flies spend ~70 to 80% of their day sleeping (Fig. 1E). We used these two general features of sleep under LD conditions, the presence of two daily peaks in the periodogram (at 12- and 24-h under LD) with approximately 75% of time spent sleeping within a 24-h cycle, to develop our two-process model of fly sleep.

Formulating the *Drosophila* two-process model

Although the original two-process model described above (Fig. 1A) produces a single daily peak of sleep, some animals, including humans, often display biphasic sleep with a nap during mid-day and deeper sleep during the night, much like sleep in *Drosophila* [15,45]. S- and C-process parameters that could produce bimodal sleep (e.g., daytime, and nighttime sleep episodes) were identified in an earlier two-process model (Fig. 2A) [5]. We therefore began building our model with previously published parameter values defining the C-process that were shown to produce bimodal sleep and created various models consisting of different combinations of build-up and

decay rates of sleep pressure (see Suppl. Fig. 1). S-process parameters were determined in humans using EEG-based measures of sleep states [5]. In the absence of recognized physiological correlates of fly sleep, the use of behavioral inactivity was the only method by which we could estimate homeostatic parameters in this system. For each of these models we first asked if they produced unimodal, bimodal, complex, or arrhythmic sleep patterns (see Suppl. Fig. 1). We found that a large region of the parameter space of S-process (all values that S can have, as defined by the input to the model) produced complex sleep rhythms (Fig. 2B), meaning they produced periodograms with three or more peaks above the significance line. A significant region of the parameter space failed to produce coherent sleep rhythms (Fig. 2B), meaning that there were no detectable periodicities revealed by our χ^2 analysis. Small regions of the parameter space produced coherent unimodal (one 24-h periodogram peak) or bimodal (peaks at 12-h and 24-h) sleep rhythms (Fig. 2B).

Given that we were interested in parameter values that produce two daily episodes of sleep, we focused on combinations that yielded two periodogram peaks. Among these, we quantified the percentage of time spent sleeping per cycle. For each set of parameters, we then compared the values they produced with the percent of time that three fly genotypes, *Canton-S*, w^{1118} and *yw*, slept per cycle (median over all flies/genotype), using sum of squared differences (SSD; see Materials and Methods; Fig. 2C). We found that the lowest SSD (best fit) was attained when the value for the build-up of sleep pressure was 0.91 and the decay of sleep pressure was 0.94 (Fig. 2C). Therefore, we chose these parameter values as the best descriptors for daily fly sleep under standard LD cycles. The model generated using these parameter values is shown in Fig. 2D. Though it appears to underestimate daytime sleep and somewhat overestimate nighttime sleep, the

percentage time spent sleeping/24-h cycle predicted by the model was ~80%, which is close to the percentage of time that the three fly strains spend asleep (Fig. 2E).

Predictions from the two-process model

We built a two-process model of *Drosophila* sleep to systematically predict the effects of altering either the S- or the C-process on fly sleep rhythms. We first asked what would happen to daily sleep if the circadian modulation of sleep thresholds were abolished. To model this, we set the amplitude of the upper and lower thresholds to zero, such that they were held constant at their mean values. Our model made the straightforward prediction that eliminating the contribution of the circadian system would result in ultradian sleep rhythms (Figs. 3A and B). Ultradian rhythms in the locomotor activity of flies with no functional circadian clocks have been reported previously [46,47]. Our model suggests that such rhythms are a predictable consequence of a functional S-process in the absence of circadian modulation of sleep thresholds and predicts ultradian periodicities of sleep of eight- to nine-hours per cycle in the absence of a functional circadian clock. We tested this prediction by examining sleep rhythms in wildtype and various loss-of-function clock mutants (*per*^{01}, *tim*^{01}, *clk*^{JRK} *and cyc*^{01}) under constant darkness using continuous wavelet transforms (CWT; a method to detect wide range of periodicities at local timescales) as have been used previously for circadian time-series data (see Materials and Methods) [48–51].

We found strong 12- and 24-h periodicity in the sleep rhythms of wildtype (*CS*) flies, as expected (representative CWT spectrograms in Fig. 3C), along with weak ultradian components around seven to eight hours (Fig. 3E). As expected, there were no detectable periodicities in the circadian range for any of the clock mutants (representative CWT spectrograms in Fig. 3D). However, there

was a broad distribution of ultradian periodicities ranging predominantly from ~two to ten hours (Figs. 3D and E) in these flies that were apparent in raw sleep time-series (example shown for *per*^{01} flies in Suppl. Fig. 2). The range of ultradian periodicities that we detected for sleep was similar to those detected previously for locomotor activity [46,47], though there was considerable inter-strain variation in the width of the distribution for the clock mutants (Fig. 3E). Our results indicate that sleep/wakefulness rhythms are indeed ultradian and likely driven by a functional S-process in the absence of circadian clock-controlled thresholds. We think that this provides a more parsimonious explanation for the presence of ultradian rhythms in activity than the uncoupling of endogenous ultradian oscillators in loss of function clock mutants [46,47,52].

How independent are the S- and C-processes in *Drosophila*?

Based on the persistence of the C-process in the absence of sleep and the maintenance of the S-process in the absence of circadian timekeeping, the two-process model assumes that they act without influencing one another's kinetics (reviewed in [11]). For example, rhythms in the propensity to sleep appear to be independent of the duration of prior waking or sleep duration, implying the independent action of the clock and the homeostat [31]. Furthermore, homeostatic increases in NREM sleep and slow wave activity are observed after sleep deprivation in the absence of the brain's central circadian pacemaker, the suprachiasmatic nuclei (SCN) [53–56]. Though these results support the independence of the S- and C-processes parameters, recent studies have suggested that these two processes influence one another (reviewed in [11]). For example, loss-of-function modifications to the circadian clock appear to have significant impact on sleep homeostatic markers in mice and flies [32,57–61]. Furthermore, variation in human chronotypes is associated with variation in sleep homeostatic markers (reviewed in [62]).

Thanks to the genetic tools available for the manipulation of the C-process in *Drosophila*, we were able to generate flies with a wide range of circadian periodicities and assess the relationships between the period of the C-process and the amount and waveform of sleep. Thus, we can compare the model's predictions to the experimental effects of C-process manipulation on sleep rhythms (Fig. 4A). We first made predictions about the power of sleep rhythms across a wide range of free-running periods (Fig. 4B) by altering the free-running periods of the upper and lower thresholds in our model (see Materials and Methods), leaving all other parameters unchanged (Fig. 4A; Suppl. Fig. 3). Our model predicted that specific ranges of free-running periodicities would be associated with relatively weak sleep rhythms (Fig. 4B). Specifically, that sleep rhythms would display relatively low periodogram powers for circadian periods between 16- and 19-h, relatively higher power for periods between 19.5 and 24-h, and relatively low power for periods between 24 and 30-h (Fig. 4). Interestingly, power was predicted to be relatively high again at periods longer than 30.5-h (Fig. 4B). We then determined the amount of time spent sleeping/circadian minute for this entire range of circadian periods. We scaled sleep to circadian minutes to account for the difference in the total number of circadian sleep cycles that different free-running periods would complete for a fixed simulation time (see Materials and Methods). Our model produced the straightforward prediction that the proportion of time spent sleeping would increase linearly with lengthening of circadian period (Fig. 5B; see subsequent sections). Despite the simple nature of this prediction and its significant implications for circadian sleep regulations, no previous work to our knowledge has recognized or experimentally tested it.

To test the model's predictions, we recorded locomotor activity in flies with a wide range of circadian periods under DD and constant temperature conditions. We employed five *period* alleles (located on the X-chromosome): per^T (free-running period – 15-h; [63]), per^S (free-running period – 21-h; [64]), per^+ (free-running period – 23.5-h), per^L (free-running period – 27.75-h; [64]) and per^{01} (arrhythmic; [64]). As expected, these alleles produce significantly different free-running periods (see Table 2). By creating all possible combinations of these alleles (by including heterozygous females), we generated large numbers of flies with a continuous and wide range of free-running circadian periods between ~15- to ~30-h, as previously described by others (see Table 2; [63,64]). We performed this experiment twice, pooled flies from both experiments, and quantified power and percentage time spent sleeping for all rhythmic flies observed (Tables 2 and 3).

The sleep rhythms displayed by these flies revealed relatively weak power in flies with free-running periods between 15- and ~17-h (Fig. 4C). Power was relatively high for flies with periods between 19- and 25-h. Power dropped as periods increased beyond 25-h and increased again for periods between 27- and 30-h before falling again for longer periods (Fig. 4C). Thus, the model qualitatively predicted a dependence of sleep rhythm power on free-running period (Figs. 4B and 5A), though the specific ranges of periods associated with weak sleep rhythms were not predicted precisely (Fig. 5A). We also quantified the relationship between free-running period and the power of locomotor activity rhythms. Interestingly, we found that there is a reasonable match in normalized power of rhythm between locomotor activity and sleep time-series in the short period range (between ~15- to ~21-h), but there is quite a mismatch for period values beyond ~21-h (Suppl. Fig. 4A). Consequently, the degree of match between power of locomotor activity time-

series and predictions from the model is different from that with sleep time-series (compare Figs. 5A and Suppl. Fig. 4B), thereby highlighting the importance of using sleep time-series to study the circadian regulation of sleep rather than extrapolate from periodogram analyses on locomotor activity time-series. Furthermore, this quantitative relationship between free-running period and power of sleep rhythms was not a consequence of the limitations of the Chi-square periodogram. Analysis using the Lomb-Scargle periodogram revealed a similar relationship between period and power (Suppl. Fig. 5).

Interestingly, the amount of time spent sleeping/circadian minute seems to increase with lengthening free-running period as predicted, but, in contrast to predictions, they do so in a non-linear manner (Figs. 4D and 5B), with an unpredicted dip in the amount of time spent sleeping for a narrow range of periods around ~18-h, after which it increases until a small dip at periods around 26-h (Figs. 4D and 5B). These dips were not predicted by the model (Fig. 5B), which predicted a somewhat linear increase in proportion of time spent sleeping with lengthening free-running period (Fig. 5B). The model also tended to overestimate the time spent sleeping compared to the sleep measured in flies (Fig. 5B).

As discussed above, although the S- and C-processes were initially thought to act without influencing each other's kinetics [31], recent work indicates that they do in fact influence each other [11,32,57–62]. We therefore sought to adjust the S-process parameters for each free-running period to maximize the fit with our experimental data, once again using the SSD-based approach (Fig. 5C; also see Suppl. Fig. 6) thereby producing a much better fit for power and amount of time spent sleeping between the model and experimental results (see Materials and Methods; Figs. 5D

and 5E). The S-process values that produce this fit are shown in Figs. 6A and 6B. The relationship between these S-process values and free-running period are complex and non-linear (Fig. 6). Our adjusted model suggests that the build-up of sleep pressure is increased for periods between 16.5- and 19.5-h (Fig. 6A). For periods of 20-h and longer, our model indicates that S build-up rates are more or less constant until period of ~30-h, at which point the model predicts a small dip (Fig. 6A). Our simulation routine also suggests that the rate of sleep pressure decay falls between periods of 15- and 21-h, beyond which it increases and stabilizes at around 24-h (Fig. 6B). Though a simple two-process model, in which the S- and C-processes are assumed to act without an inter-relationship in their parameters, *qualitatively* captures a remarkable number of features of fly sleep, our analyses predict that the rates of the two processes are indeed interdependent in a way that has implications for our understanding of the regulation of *Drosophila* sleep.

To what extent is *Drosophila* sleep a unitary state?

The original two-process model made predictions regarding the amount of total sleep time by modeling the S-process based on the exponential decay of the power of sleep EEG (0.75- to 25-Hz). This wide range of EEG frequencies corresponds to all sleep types, i.e., slow wave and REM sleep. Interestingly, the decay constant derived from such a wide range of EEG frequencies was very similar to the constant derived from slow wave sleep alone (0.5- to 2-Hz) [5,65], thereby suggesting that although the two-process model accounts for total sleep, the S-process properties are most closely reflected by NREM sleep.

Though sleep has largely been treated as a unitary state in the fly, several independent approaches support the notion that long durations of inactivity correspond to a relatively “deep-sleep” stage

[33–39]. For example, metabolic rates of flies that have been inactive for ~35-min are significantly lower than flies that have been inactive for the standard five-minute definition of fly sleep [33]. Furthermore, experiments tracking arousal thresholds and brain physiology identify deeper sleep intensities when flies have been inactive for ~30-min [34]. Since decay constants best reflect NREM sleep, we assessed the degree to which model predictions would describe empirical data when increasing durations of inactivity were used as the defining criterion for a sleep like state, thereby biasing our sleep analysis to longer, presumably deeper, bouts of sleep in experimental flies. Because recent studies in flies (discussed above) have established a clear correlation between the duration of inactivity and the depth of sleep, we use the term "deep" to refer to sleep bouts that are longer than the traditional unitary five-minute inactivity definition of fly sleep. Similar associations between sleep consolidation (number of spontaneous brief awakenings) and sleep pressure (measured using slow wave activity) have also been reported in rodent models [66], therefore suggesting that this association is likely a conserved phenomenon.

We systematically altered the inactivity duration definition of sleep, i.e., the duration of inactivity used to define the sleep state and examined the correlation between the amount of time flies spent sleeping and our model's prediction (Figs. 7A-B). Traditionally, any bout of inactivity that is five minutes or more is defined, in flies, as sleep. The correlation between our model's prediction and measurements of amount of time spent sleeping in our series of allelic combinations of *period* changes very little with increasing inactivity definitions, at least until the criterion for sleep reaches 30-min of inactivity (Figs. 7A-B). This result implies that shorter bouts of inactivity contribute very little to how the amount of time spent sleeping varies with circadian period.

To further test this idea, we performed the same analysis as above but with specific ranges of inactivity durations used for the definition of sleep (see Materials and Methods for details). Briefly, a five to 30-minute interval definition of sleep would mean that any bout of inactivity that is equal to or more than five minutes but fewer than 30 minutes would be considered sleep. We found that the correlation between empirical results and model predictions is relatively low when five to 30 minutes of inactivity were used as the definitions of sleep (Fig. 7B). Correlations improved a little when the inactivity definition was set to 30 to 60-minutes and became almost as high as the standard definition of sleep (five minutes or longer) when set to 30 to 120 (Fig. 7B). These results are consistent with recent work suggesting that different durations of inactivity are unlikely to represent the same state with respect to sleep in *Drosophila* [33–39].

Inactivity bouts longer than 30-min reflect the S-process more closely than the standard definition of fly sleep

As discussed above, our results suggest that homeostatic S-processes in the absence of a functional circadian clock are expected to produce ultradian sleep rhythms (Fig. 3). If longer bouts of inactivity better reflect the S-process than the standard definition of fly sleep, these ultradian rhythms would be unaltered in loss-of-function clock mutants when longer durations of inactivity are used to define sleep. This prediction stems from the idea that shorter bouts of inactivity are dispensable for the observed temporal patterns of sleep behavior. Indeed, we found that ultradian periodicities in sleep rhythms are observed even when inactivity duration definitions of up to 30 minutes of inactivity are used for sleep (Figs. 7C and 7D). When we examined the CWT spectrograms for wildtype *CS* flies, it is clear that, as expected from decades of previous work, 12- and 24-h components strongly dominate the range of periodicities detected under DD (Figs. 7C

and 7D). In contrast, there was a much larger number of times ultradian periodicities were detected in the *per*^{01} flies (Figs. 7C and 7D). Interestingly, when we examined the 30-min definition of sleep in *per*^{01}, there is a more uniform and broad distribution of ultradian periodicities (Fig. 7D). This is suggestive of the fact that the inclusion of all sleep bouts may obscure ultradian rhythms of longer, presumably deeper, sleep bouts. Our results further strengthen the notion, recently proposed by others [33–39], that sleep is not a unitary state in flies. Our analysis suggests that such longer bouts of inactivity are likely the best reflection of S-process action.

Long bout sleep has distinct temporal organization

Next, we asked if and how biasing our analyses to long-bout (presumably deeper) sleep alone would affect the temporal organization of sleep in wild-type flies under LD and DD conditions. Environmental light promotes arousal and, when very bright, can suppress locomotor activity in flies (e.g., [67]). We therefore compared the temporal distribution of sleep across three entrained day and night cycles and across four subjective days and nights under DD, using varying inactivity duration criteria for sleep (Fig. 8A). As previously shown, the standard definition of sleep reveals two episodes of sleep per cycle under both LD and DD conditions (Fig. 8A), although this is less pronounced in DD [68]. Interestingly, increasing the inactivity duration criterion for sleep produced no major effect on the timing of sleep under LD, but resulted in a near complete loss of sleep during the subjective day under DD (Fig. 8A). In other words, under free-running conditions the longest bouts of inactivity/sleep occur predominantly during the subjective night. Thus, the temporal regulation of short duration and long duration bouts of sleep appear to be different in the absence of an environmental cycle, suggesting that the circadian system likely regulates shallow and deep sleep differently.

To examine this further, we also compared sleep of two different sleep definitions, i.e., 5-min and 30-min in *CS* flies under a longer experiment of 15 days under DD. We found that even under prolonged DD, subjective nighttime sleep is almost identical for long-bout sleep, but subjective daytime long-bout sleep is drastically reduced (Fig. 8B). This result is consistent with previous work showing that subjective nighttime rest bouts are predominantly longer than 30 minutes [12]. It is also important to note that for relatively long inactivity duration criteria for sleep, the mean and median profiles of sleep begin to diverge significantly, which is not seen for the standard definition of sleep (five minutes of inactivity or more). This is important to consider because averages may not be representative of central population tendencies when longer bouts of inactivity are considered [69]. The clear difference between the temporal organization of standard measures of fly sleep and longer bouts of sleep under constant darkness is consistent with the notion that short and long bouts of inactivity represent different kinds of sleep that are subject to distinct modes of regulation.

An independent test confirms that faster running clocks also have altered homeostatic properties

In fitting our two-process model to sleep observed over a range of circadian periods, our results indicate that, as previously suggested, the S- and C-processes interact, with changes in the S-process predicted to accompany changes in the free-running period of the C-process. For example, we increased the fit of our model by changing the rates of S-process increases and decreases as a function of free-running period (Figs. 5 and 6). We therefore sought to examine the rates of build-up and decay of the homeostatic sleep pressure in flies with different free-running circadian

periods. The relatively high values of S-process build-up and lower values of S-process decay, both of which correspond to faster rates of build-up and decay (see Fig. 6), for flies with free-running periods around 20-h, suggest that flies with these circadian periods will display sharper increases and declines in sleep pressure compared to flies with longer periods (Figs. 6C and 6D). To look at this relationship more closely we examined per^{+} and per^{S} flies under conditions in which the C-process had been rendered arrhythmic, a condition which reveals ultradian rhythms driven by the operation of process S alone (Fig. 3). Although there was no statistically significant difference in the adjusted rates of build-up of sleep pressure between these two genotypes in our best fit model, our adjustments revealed that per^{S} flies have a significantly faster decay of sleep pressure than per^{+} (Fig. 6). This leads to the following predictions in the absence of circadian cycling of sleep thresholds (therefore, no circadian gating of sleep): (i) ultradian rhythms in sleep/wake will be faster in per^{s} mutants compared to per^{+} flies, (ii) total amount of sleep would be lower, and (iii) number of sleep bouts will be higher in per^{S} flies per unit time (Fig. 9A).

Drosophila is arrhythmic under continuous white light (LL) owing to the constitutive CRYPTOCHROME mediated degradation of TIMELESS [70–72]. Thus, LL conditions provide a convenient means of abolishing the cycling of sleep thresholds (C-process). We therefore examined sleep behavior in per^{S} and per^{+} (*CS*) flies under LL and examined longer bouts (presumably deeper, homeostatic) of sleep (Fig. 9A). As expected, over the duration of 15 days under constant white light, there was a clear absence of any circadian rhythmicity in both *CS* and per^{S} flies (Fig. 9B). Employing recently described methods [73,74], we identified three specific bands of ultradian periodicities using Discrete Wavelet Transforms (see Methods) that account for the majority of spectral variance in the sleep timeseries of *CS* and per^{S} flies (Figs. 9C and 9D).

These three ranges of periods were 1.07-2.1-h (τ_s *or* τ_{short}), 2.1-4.27-h (τ_m *or* τ_{medium}) and 4.27-8.53-h (τ_l *or* τ_{long}; Figs. 9C and 9D). We analyzed the values of period in these categories separately for both these strains. We found that indeed per^S had significantly faster ultradian periods in the τ_s category (Fig. 9E). There was no significant between-strain difference in periods in the other two period categories (Fig. 9E). Furthermore, we found statistically significantly reduced total sleep (Fig. 9F) and increased bout numbers (Fig. 9G) in per^S flies compared to *CS* flies. Our results, therefore, support *all three* predictions from the model, thereby lending support to the notion that shorter free-running periods are indeed associated with faster rates of change of the sleep homeostat (particularly, decay rates).

Discussion

Through this manuscript, we show that an examination of the circadian regulation of sleep must involve the use of time-series analyses on sleep data instead rather than relying on locomotor activity data (Fig. 1). We have created tools to make such analyses accessible to a wider community of sleep researchers through an open-access R package [40] (different from our recently published MATLAB software, PHASE [75]; https://cran.r-project.org/web/packages/phase/index.html). We also show that a simple two-process model with can explain multiple aspects of *Drosophila* sleep remarkably well (Figs. 2-5). However, covarying sleep homeostatic parameters along with the free-running period produces much better fits with experimental observations (Figs. 5C-E) and suggests a non-linear and complex relationship between S-process parameters and the circadian clock speed (Figs. 6 and 9). Furthermore, we show that the fits between predicted values from the model simulations and experimental values are only very slightly dependent on short bouts of sleep, thereby indicating that longer bouts likely

provide the clearest reflection of the S-process in flies (Fig. 7), and that they likely have distinct temporal regulation (Fig. 8). These results support the utility of a formal two-process model for understanding the regulation of sleep in *Drosophila*.

How does fly sleep compare to sleep across the animal kingdom?

To gain perspective on how *Drosophila* compares to other animal species, we compared the percentage of time that flies spend sleeping to a wide range of animal taxa (Suppl. Fig. 7). Most of this data set was curated from a comprehensive review by Campbell and Tobler (1984) [1]. The remaining data were collected by a separate literature survey [76–84]. In all, we compared fly sleep to sleep in 187 species/populations (which includes *Drosophila* species from different geographical locations, other non-*Drosophila* invertebrates, non-mammalian vertebrates and mammals). There is a large variation in amount of sleep within the *melanogaster* species itself, depending on their geographical origin [84]. When using the standard definition of sleep, *CS* flies from our laboratory sleep more than that of 174 of these species/populations (Suppl. Fig. 7), 50% of which are asleep for ~30 to ~60% of the day (Suppl. Fig. 7). If we define sleep as 30-min or more or 60-min or more of inactivity, a definition that fits the S-process well in our model, flies sleep for ~53% and ~40% of the day, respectively, which would place flies closer to the middle of the distribution of sleep amount for the animal species surveyed here (Suppl. Fig. 7).

It is important to note that it is challenging to directly compare the percentage of time spent asleep across such a wide range of taxa, given that a wide range of methods were used to measure sleep. However, in case of bats and opossums, which are among the animals that sleep more than our laboratory's *CS* flies in this survey, the basis of the sleep measurement was physiological

recordings [1]. Therefore, large proportions of time spent asleep are not necessarily a reflection of the use of inactivity to infer sleep amounts. Therefore, while it is possible that *Drosophila* as a genus is a long sleeping group, the close match of longer bouts of inactivity to S-process-driven sleep (Figs. 7 and 9), and the amount of long bout sleep relative to other groups (in Suppl. Fig. 7) suggest that such long duration may be more akin to sleep like states in other species than the current definition of fly sleep widely employed by the field.

On ultradian rhythms in sleep and the inter-relationship between circadian period and rates of homeostatic processes

The theoretical framework around Borbély and Daan's two-process models has played a critical role in the advances made in our understanding of mammalian sleep [2,4–7]. The conservation of sleep-like states across taxa and the power of *Drosophila* as a genetically tractable organism has made the fly a fruitful model system for the study of sleep regulation. However, the field of fly sleep has not benefitted from the strong theoretical framework provided by a formal two-process model. The utility of this model as a framework for the investigation of fly sleep is exemplified by its prediction that ultradian sleep rhythms are a consequence of a functional S process in absence of oscillating thresholds (Figs. 3A and 3B). Although simple, this prediction, to the best of our knowledge, has not been directly tested in any animal model as an outcome of the two-process model.

Though we are the first, to our knowledge, to directly test for the presence of ultradian *sleep* rhythms in clock loss of function animals as a test of the two-process model, we are by no means the first to measure the presence of ultradian rhythms in animals. Indeed, the two-process model

has been adjusted to account for the presence cycling sleep states in mammals, the cycling of which produces ultradian EEG rhythms during bouts of sleep [85–87]. However, the ultradian changes in sleep state produced by normal sleep cycles occur during the circadian clock timed daily window of sleep and are therefore distinct from the ultradian rhythms in sleep bouts predicted by two-process models when the circadian cycling of sleep thresholds is abolished. Furthermore, Mistlberger and co-workers (1983) [88] detected the presence of ultradian rhythms in wheel running activity when the suprachiasmatic nuclei were bilaterally ablated, thereby abolishing circadian timekeeping. However, these ultradian rhythms were not predicted in the context of the two-process model.

Previous work on loss-of-function *period* mutants detected the presence of ultradian rhythms in locomotor activity [46,47], which were hypothesized to be due to an uncoupling of ultradian oscillators [46,52,89]. However, our results, which demonstrate the presence of such rhythms in a range of loss-of-function clock mutants (Figs. 3D and 3E), suggest that they are a simple consequence of the rise and fall of sleep pressure between non-oscillating sleep thresholds, akin to an hourglass system as has been previously suggested [90]. It is important to note here that although the model predicts an ultradian sleep rhythm of ~eight to ~nine hours, our results in clock mutant flies reveal much ultradian shorter periods, albeit with a wide distribution of periods that lack the stability of a robust circadian oscillator. Among the possible explanations for this discrepancy are a reduced distance between the thresholds in the mutants, a steeper rise or decay of sleep pressure, or non-oscillating but unstable thresholds in loss of function clock mutants. The large variance in ultradian periodicities that are detected may also be a consequence of independent stochastic fluctuations of the upper and lower thresholds and the distance between them. Indeed,

a combination of all such factors may be at play. Moreover, enhanced sensitivity of *per*^{01} mutants to sleep deprivation has been reported previously, suggesting a pleiotropic effect of the loss of *period* on the sleep homeostat [32]. Similar pleiotropic effects may also govern the S-process of other loss of function clock mutants, contributing to this large variation in detected ultradian periodicities. However, the detectable presence of such ultradian oscillations in sleep (Figs. 3 and 7) and the possibility of detailed characterization of their properties (Fig. 9) under conditions of non-cycling upper and lower thresholds promises to be a useful new approach for the study of the mechanisms regulating process S that are highly likely to complement work employing sleep deprivation to examine the homeostatic regulation of sleep.

The detectable effects of faster decay of sleep pressure in *per*^{S} flies under LL conditions (Fig. 9) is remarkable because PER protein is constitutively low under continuous light [91]. This implies that there may be a fundamental relationship between clock speed and the rates of change of the sleep homeostatic system. It is possible that the free-running circadian period present during development shapes homeostatic systems so as to coordinate the build-up and/or decay of sleep pressure with clock speed. It is also possible that *period* alleles have different effects on the homeostatic control of sleep via epigenetic mechanisms. Recent studies have reported differential epigenetic regulation associated with cell populations with divergent periods and distinct levels of clock gene expression [92,93]. Our results in flies may be broadly relevant to animal sleep regulation, as similar results have been reported in humans [62]. Specifically, the human *PER3*$^{5/5}$ polymorphism is highly enriched in morning chronotypes, and such early types also have faster running circadian clocks. Remarkably, *PER3*$^{5/5}$ individuals experience higher sleep pressures and

a faster build-up of non-REM activity during sleep deprivation compared to another human *PER* polymorphism, *PER3*$^{4/4}$ [62,94].

Previous studies that simulated S-process parameters in rodent models found considerable variation in the time constants of build-up and decay rates of the homeostatic sleep drive across species and among strains of the same species [5,95,96]. We compared these values and the time constants derived from human EEG data and found that rodent models have faster build-up and decay rates of the S-process compared to humans. We then looked at free-running periods of a commonly used mouse strain and that of humans and found that mice have faster running circadian clocks than humans [97,98]. This is consistent with our conclusion that speed of the circadian clock likely affects the rates of S-process increases and decreases. Lab populations of *D. melanogaster* typically have shorter than 24-h periods under constant darkness as opposed to humans who have longer than 24-h periods [98,99]. When we compared the best fitting S-process rates between flies and humans, we find that the build-up rates are indeed faster for flies, consistent with our hypothesis. Interestingly however, the decay rate was slower. We speculate that this may be necessary for facilitating two bouts of sleep/cycle, where one bout is considerably longer than the other.

The utility of the two-process model of fly sleep for understanding previous findings and the generation of new testable hypotheses

The integration of this quantitative model with previous work examining the effects of specific clock neuron types on sleep and the daily timing of neural activity they display, offers a unique and powerful framework for understanding the neural basis of circadian sleep regulation in the fly.

An examination of our model in the context of the growing body of knowledge regarding the relationships between circadian clock neurons and sleep timing leads to specific and empirically testable hypotheses that have not emerged from current models. Furthermore, the roles of circadian clock neurons in sleep control have not been investigated in the context of cycling sleep thresholds.

Under normal circumstances (i.e., the absence of physiological or social challenges), the model suggests that the onset of daytime and nighttime bouts of sleep are timed by the rising phase of the upper threshold (Fig. 10A). Furthermore, the model suggests that the timing of morning and afternoon waking are both regulated by the rising phase of the lower threshold (Fig. 10A). Finally, the falling phase of the lower threshold is predicted to play an important role in the maintenance of nighttime sleep (Fig. 10A). For the sake of simplicity, we assume that the upper and lower thresholds are regulated in unison by the circadian clock neuron network, with a constant distance between them. Work over the last decade has assigned sleep- or wake-promoting functions to specific classes of circadian clock neurons (reviewed in [14]). For example, the small ventral lateral neurons (s-LNvs) and the dorsal lateral neurons (LNds) are thought to be wake-promoting, whereas the dorsal neuron 3 class (DN-3) is thought to be sleep-promoting (reviewed in [14,16]). In these cases, the daily timing of neural activity displayed by these cell types, as measured by relative Ca^{2+} levels, fits these proposed roles in sleep control well (Fig. 10A).

The s-LNvs display Ca^{2+} peaks that coincide with the morning bout of locomotor activity, the LNds display peaks that coincide with the evening bout of locomotor activity, and the DN-3s display their highest Ca^{2+} levels during the nighttime bout of sleep [100]. Integrating these patterns

with our two-process model suggests that the s-LNvs control the timing of morning wakefulness by driving the initial rise of the lower sleep threshold, that the LNds promote the timing of evening wakefulness by the continued rise in the in the lower sleep threshold, and that the DN-3s promote the maintenance of nighttime sleep by driving the fall of the lower threshold throughout the night (Fig. 10A). Though we opted for a simple model for the rise and fall of the upper and lower threshold and have proposed that the action of specific subsets of clock neurons contribute either to the rise or fall of both, the model also suggests that the timing and duration of daytime and nighttime sleep windows could be controlled in other ways. For example, the distance between the two thresholds, the phase relationships between the two thresholds, or the relative amplitudes of the upper and lower threshold cycles might all be modulated by the circadian system to shape the timing and amount of sleep.

To further examine how changes in the circadian system might affect sleep regulation, we ran our model with a C-process that fell every day at the normal times and to the normal extent but that failed to rise above the previous mean value (Fig. 10C; left). This scenario is taken to represent the absence of the wake-promoting effects of LN function in our synthesis. In this case, the model predicts modest changes in the sleep rhythm, with negligible weakening of the sleep rhythm, a minor increase in total sleep, and a rebalancing of sleep between the subjective day and subjective night, with daytime sleep increasing and nighttime sleep decreasing (Fig. 10C). We next ran our model with a C-process that rose every day at the normal times and to the normal extent but failed to fall below the previous mean value (Fig. 10C; right). This scenario is taken to represent the absence of the sleep-promoting effects of DN function in our model. In this case the prediction was starkly different: rhythms of homeostatically-controlled (i.e., long-bout) sleep were predicted

to be arrhythmic. Similarly opposing predictions were made by models in which rises or falls in sleep thresholds were maintained but reduced: changes to C-process rises produced modest effects on sleep rhythms (Fig. 10C), while changes to C-process falls produced a significant weakening of the predicted sleep rhythm (Fig. 10C).

In addition to generating the above testable hypotheses regarding the specific roles of circadian clock neurons in the regulation of daytime and nighttime sleep, our integration of the model with previously published Ca^{2+} rhythms may reconcile previously conflicting results. Several studies have come to opposing conclusions regarding the role of the dorsal neurons 1 (DN-1) in sleep regulation: they have been proposed to be both wake- [101,102] and sleep-promoting [103,104]. Though these apparently incompatible conclusions may ultimately be explained by the different technical approaches used in these studies, the two-process model provides an explanation for how similar experimental manipulations of the same clock neuron classes might lead to contradictory conclusions. According to Liang et al., 2016 [100] the DN1ps display peak levels of neuronal activity in the middle of the night, a time associated with nighttime sleep, a pattern that would appear to fit a sleep promoting role for these clock neurons. However, our model predicts that the effect of acutely exciting the DN-1ps would depend on the timing of the manipulation on neural signaling. For instance, if the DN-1ps promote the fall in upper and lower sleep thresholds, as suggested by the relationship between the sleep thresholds and DN-1p Ca^{2+} profiles (Fig. 10A), exciting these neurons during the late afternoon would lead to an early and prolonged fall in thresholds (Fig. 10B). According to the model, this would increase daytime sleep and cause a slight delay and decrease in nighttime sleep (Fig. 10B). An increase in daytime sleep was used by Guo et al., 2016 [104] to support the conclusion that exciting DN-1ps promotes sleep. In contrast,

Kunst et al., 2014 [102], present evidence for increased daytime sleep (Fig. 10B), but also describe a reduction in nighttime sleep, which, while not observed by Guo et al., 2016 [104], is predicted by our synthesis. Blocking synaptic transmission in the DN-1ps has been shown to decrease sleep [104]. If we assume that this manipulation results in sustaining sleep thresholds at high levels, our synthesis predicts this effect as well (Suppl. Fig. 8).

Speculations and Concluding Remarks

Our time-series analysis of *Drosophila* sleep detected the presence of ultradian periodicities under constant conditions in both wildtype flies and mutants lacking circadian timekeeping. In wild-type flies these ultradian rhythms were dwarfed by the presence of strong circadian gating of sleep/wake cycles that produce the characteristic 12- and 24-h periodicities seen in normal sleep cycles in the fly (Figs. 3C and 3E). Might these relatively weak ultradian sleep rhythms reflect a cycling through different stages during the two daily bouts of sleep? Might such cycling occur at specific times of the circadian cycle? Answers to these questions await further detailed analyses of sleep time-series using the methods of analysis described here, all of which are freely available.

Here we have synthesized a formal, quantitative model of sleep regulation in *Drosophila* and have used it to guide the development of empirically testable hypotheses regarding the circadian control of sleep. We've also made this accessible to the wider sleep community by generating a Shiny-based GUI to facilitate simulations. We propose that this model can serve as a powerful framework for investigating the contributions of the various clock neuron to sleep regulation. The predictions made by this model were supported by experimental results, which are reminiscent of human studies on the relationships between circadian timekeeping and the homeostatic control of sleep.

This suggests that the relationships between these two processes discovered in the fly will prove to be broadly relevant to our understanding of sleep regulation in animals. Our analysis also suggests that simple changes to the way we define sleep-like states will support significant insights into the homeostatic regulation of fly sleep. Because the two-process model has been a major driving force for our understanding of sleep regulation in humans, we propose that adopting the two-process model to other genetically tractable experimental systems will support significant new insights into the mechanisms controlling sleep.

Materials and Methods

Fly husbandry

Canton-S (CS; BDSC stock number: 64349*)*, *white*^{1118} (*w*^{1118}; [105]), *yellow, white* (*yw*; BDSC stock number: 1495), *period*^{TAU} (*per*^{T}; [63]), *period*^{SHORT} (*per*^{S}; [64]), *period*^{LONG} (*per*^{L}; [64]), and *period*^{01} (*per*^{01}; BDSC stock number: 80928), *timeless*^{01} (*tim*^{01}; BDSC stock number: 80930), *clock*^{JRK} (*clk*^{JRK}; BDSC stock number: 80927) and *cycle*^{01} (*cyc*^{01}; BDSC stock number: 80929) flies were used for the behavioral experiments reported in this manuscript. *CS* flies are also referred to as *period*$^{+}$ (*per*$^{+}$) throughout the text, as all the *period* alleles used here were in a *CS* background. Flies were reared on Corn Syrup/Soy media made by Archon Scientific (Durham, North Carolina). Flies were approximately five days old on day one of all behavioral experiments.

Generation of flies with a wide range of free-running periods

For the generation of flies with a wide range of period values, virgin females, and males from all five *period* allele cultures (*per*^{T}, *per*^{S}, *per*$^{+}$, *per*^{L} and *per*^{01}) were collected over the span of approximately five days. Reciprocal crosses were performed, resulting in a total of 25 distinct

crosses. Male and female offspring from each of these 25 crosses, representing 50 distinct sex and genotype combinations (see Tables 1 and 2), were collected and assayed for locomotor activity as described below.

Assay of locomotor activity

Locomotor activity was recorded using the *Drosophila* Activity Monitor (DAM) system (Trikinetics, Waltham, MA; https://trikinetics.com). Beam crossing counts were collected every minute for all experiments. Flies were recorded under LD12:12 cycles, constant darkness (DD) or constant bright white light (LL). In all experiments reported in this manuscript, flies were assayed under 25 °C and the intensity of white light was between ~400 and ~500 lux.

Data analyses and visualization

Circadian time-series analysis of Drosophila sleep

Locomotor activity of approximately 32 each of *CS*, w^{1118} and *yw* male flies was recorded under LD12:12 for nine days, after which activity was recorded under constant darkness (DD) for seven days. Beam crossing data from these recordings were used to determine the pattern and amount sleep for each fly. Individual fly locomotor activity and sleep time-series data, binned in 1-minute intervals, were subjected to (Chi-squared) χ^2 periodogram analyses. To visualize sleep profiles as averaged time-series, flies from three independent experiments under LD12:12 were pooled, which included more than 90 flies for each genotype.

Calculating the percentage/amount of time spent sleeping

For fly sleep under LD cycles in this study, the percentage of time spent sleeping was calculated by first computing the total sleep over the entire duration of the experiment for each fly (last four cycles of entrainment). This total was divided by the number of 24-h cycles (i.e., 4), and then multiplied by $\frac{100}{24}$.

Percentage of time spent sleeping for other species were computed based on the number of hours of sleep reported in Campbell and Tobler (1984) [1]. In addition, sleep amounts were estimated from published figures for a few other species whose sleep has been more recently quantified [76–81]. In all these cases the averaged/reported amount of sleep is multiplied by $\frac{100}{24}$.

For flies under DD in this study and for simulations of free-running sleep, the total amount of sleep (in minutes) over the entire duration of the experiment or simulations (for each fly in case of the experiment) was calculated. Because flies with different free-running periods would differ in the number of sleep/wake cycles experienced during free run – for example periods shorter than 24-h would complete more than 10 cycles in 10, 24-h days and clocks with periods longer than 24-h would complete fewer – we accounted for clock speed in our calculations. We did this by estimating the number of circadian cycles each fly, or model output completed over the entire duration of the experiment/simulation. In the case of a 10-day experiment, a fly with a 23-h period would have free-run for $10 \times \frac{24}{23} = \sim 10.44$ cycles or $10.44 \times 240 \times 60 = 150336$ circadian minutes, as compared to $10 \times 240 \times 60 = 144000$ circadian minutes for a fly with a period of exactly 24-h. The proportion of a circadian minute that a fly (real or simulated) spent sleeping was then calculated as the ratio of total minutes of sleep and the total number of circadian minutes over the entire duration of the experiment/simulation.

Continuous wavelet transforms as a tool to identify ultradian rhythms in sleep

Biological oscillations are often non-stationary time-series, i.e., their amplitude and period vary significantly over time. Such variations are often not of interest when estimating period and power of circadian rhythms. However, when attempting to identifying multiple periodic components from non-stationary time-series traditional methods like the χ^2 periodogram often fail to accurately reflect the presence of multiple periodicities, especially when they are restricted to certain windows of time throughout the length of the time-series. Recently, analytical tools to resolve circadian rhythms in both the time and frequency domain (i.e., provides period and amplitude information locally over a long time-series) have been developed and utilized [48–51]. We made use of one such tool, the continuous wavelet transforms (CWT), to examine periodic components in sleep time-series of our flies. We used functions from the WaveletComp package in R, which use a Morlet mother wavelet and resolves biological time-series in the time-frequency domain [48,106]. Complex-valued wavelet transforms such as the Morlet wavelet is useful because it provides amplitude and phase over time and generally preserves information about these locally [48,106]. To assess the presence of ultradian rhythms, sleep timeseries for all our genotypes for varying definitions of sleep were calculated in bins of 60-minutes. CWT were carried out and significance of detected periodicities were tested against a null hypothesis of "no periodicity" using shuffled timeseries. The null distributions were generated based on 1000 simulations of such shuffled timeseries. In order to compare ultradian periodicities between *CS* and per^S flies under white LL, we used a modified pipeline based on recent analytical developments [74]. We first performed discrete wavelet transforms on 1-min binned sleep timeseries of both our genotypes using a Daubechies wavelet of filter length 12 using the functions from the package "wavelets" on

R [107]. We then computed the percentage of spectral variance accounted for by each level of the scale index as has been done previously [73,74]. Based on this, we identified three period bands, i.e., 1.07-2.1-h, 2.1-4.27-h and 4.27-8.53-h (Figs. 9C and 9D). In the interest of computation time, we performed the above-described continuous wavelet transforms on flies of these two genotypes using 15-min binned sleep timeseries, and the significance of detected periodicities were based on 100 simulations of shuffled timeseries. We then computed median period and power for each fly in each of the three identified period bands after accounting for edge effects [74]. These values were then used to make between genotype comparisons. Statistical significance between genotypes were tested using bootstrapped *t*-tests with 10000 bootstrap replicates and were carried out using functions from the package MKinfer on R [108].

Time-series analysis of various definitions of sleep

Traditionally, *Drosophila* sleep has been defined as any bout of inactivity (usually the absence of beam crossings in DAM monitors) that lasts five-min or more [12,13,15]. Though this method has been shown to overestimate the amount of sleep [109], its easy implementation and consistency over decades of research have made it an integral approach to measuring sleep in the fly. In addition to the traditional definition of sleep, we systematically changed the inactivity duration criterion for sleep to examine how the temporal regulation of sleep was affected by biasing our analysis to longer bouts of inactivity or specific ranges of inactivity. For example, a ten-minute inactivity duration definition of sleep would mean that any bout of inactivity lasting ten minutes or more would be considered sleep and subjected to time-series analysis, whereas a five to 20-minute definition of sleep would mean only bouts of inactivity that are more than five minutes but fewer than 20 minutes would be considered as sleep and subject to the analysis.

Statistical tests and comparisons

Correlations between the proportions of time spent sleeping predicted from the model and the proportions measured in experimental flies using various inactivity duration definitions of sleep were tested using the Pearson's product-moment correlation implemented in R [110]. Since the overall levels of sleep change as a function of the definition of sleep, all data were normalized to maxima to restrict the dynamic range of values between 0 and 1. This reduces the extent of variation in levels across both axes and therefore is better amenable to correlation analyses. Differences in ultradian periodicities under LL between genotypes were statistically compared using a one-tailed Wilcoxon's rank sum test implemented in R [110].

Figure generation

All figures were generated using custom scripts in R. We used the "wesanderson" package [111] to generate color palettes used in the figures, except in case of the acto-/somnograms, time-series plots in Fig. 1, the CWT spectrograms, and the Suppl. Figs. In these three cases, default color palettes were used to generate the plots.

Creating the two-process model and generating predictions

A major strength of the original two-process model was that it used EEG data to derive the parameter values of the sleep homeostat [4,5]. Because no equivalent physiological correlate of sleep is, as yet widely employed in flies, we relied on best-fitting approaches to find model parameters that best explain the waveform and amount of sleep in *Drosophila*. The basic structure

of the two-process model used here is taken from a two-process model proposed by Daan et al., in 1984 [5]. The upper and lower thresholds are modeled as simple sinusoidal oscillations:

$$U = M_u + A_u \cos(\omega_u t + \varphi)$$

$$L = M_l + A_l \cos(\omega_l t + \varphi)$$

U and L are the upper and lower thresholds, respectively. M_u and M_l are the mean levels around which U and L oscillate. A_u and A_l are the amplitudes of the upper and lower threshold oscillations. ω_u and ω_l are the angular velocities of the oscillations. The angular velocities are determined by the period of the oscillation, which is expressed as $\omega = \frac{2\pi}{\tau}$. τ is the period of the oscillation, which in this study, was fixed at the same value for both thresholds. φ is the phase angle by which the starting phase of the oscillations are adjusted and was likewise fixed at the same value for the upper and lower thresholds. The build-up of sleep pressure is modeled as:

$$s_t = 1 - i \times (1 - s_{t-1})$$

s_t is the value of sleep pressure at any given time t. i is the parameter determining the increase of build-up of sleep pressure. s_{t-1} is the value of sleep pressure at any given time $t - 1$. The decay of sleep pressure is modeled as:

$$s_t = \delta s_{t-1}$$

s_t is the value of sleep pressure at any given time t. δ is the decay rate of sleep pressure. s_{t-1} is the value of sleep pressure at any given time $t - 1$. The upper and lower thresholds were computed for the entire duration of the simulation, which was typically 21-days. The simulations for sleep pressure build-up and decay were performed in discrete 30-min time-steps under the following conditions: At every time-step t, the program will increase sleep pressure as long as its value at the previous time-step $(t - 1)$ was lower than the higher threshold at t. If at $t - 1$, the sleep pressure value is higher than the upper threshold at time t, the program will release the sleep

pressure at t. Sleep pressure will continue to be released (i.e., fall) until it reaches the lower threshold value at t. The window of time in the simulation where sleep pressure is being released is designated as the window of sleep. Using this window, the number of hours of sleep predicted by the model is computed for all predictions. This allows for the estimation of percentage of time sleeping across the circadian cycle. The sleep pressure time-series thus generated was subjected to χ^2 periodogram analyses to produced estimates of number of peaks in the periodogram and to assess the power of sleep rhythms. Power was defined as the height of the periodogram peak above the 0.05 significance cut-off. To facilitate easy access to predictions from these simulations, we have created a GUI which is available here:

https://abhilashlakshman.shinyapps.io/twoprocessmodel/

Measuring sum of squared differences (SSD)

The S-process parameters that best recapitulated the waveform and amount of fly sleep were estimated using a sum of squared differences approach. For each combination of sleep pressure build-up (i) and decay (δ) parameters, we asked if the model produced two coherent peaks of sleep, and, if so, we assessed the difference between the proportion of time spent sleeping predicted by the model and the proportion of time our experimental flies spent asleep and this difference was squared to remove negative values. For the results reported in Fig. 2, SSD values were calculated across the three genotypes (using population averages; therefore, there are no estimates of errors on these parameter values) and, in the case of fitting reported in Fig. 5, SSD was computed for both the amount of time spent sleeping and for the normalized power of the sleep time-series periodogram. Any prediction that is close to empirical value would have small differences with the experimental data and consequently would have low SSD values. The build-up and decay rates

that together yielded the minimum SSD were considered the best-fitting parameters for our two-process models. See Suppl. Figs. 1, 2 and 5 for a guide to the algorithms for our model outputs.

Acknowledgements

This work was supported by a grant from the National Institute of Neurological Disorders and Stroke (R01NS077933) and start-up funds provided by the State of New York. We thank Michael Rosbash, Paul Hardin, Amita Sehgal, Patrick Emery, and Ralf Stanewsky for fly lines. We would also like to thank Aliya Fisher and Matthew Ciolkowski for technical support. We are grateful to Bill Joiner, Joydeep De, and Meilin Wu for useful discussions of the work presented in this study. Finally, we thank Maria de la Paz Fernández, Matthew Ciolkowski, Budha Chowdhury, and Robert Veline for providing useful feedback on the manuscript. We would also like to extend our thanks to four anonymous reviewers for carefully reading a previous version of this study and providing valuable feedback.

References

[1] Campbell SS, Tobler I. Animal sleep: A review of sleep duration across phylogeny. Neurosci Biobehav Rev 1984;8. https://doi.org/10.1016/0149-7634(84)90054-X.

[2] Alexander Borbély. A two process model of sleep regulation. Hum Neurobiol 1982.

[3] Moore-Ede MC, Czeisler CA. Mathematical models of the circadian sleep-wake cycle. New York: Raven Press; 1984.

[4] Serge Daan, Domien Beersma. Circadian gating of human sleep-wake cycles. In: Moore-Ede MC, Czeisler CA, editors. Mathematical models of the circadian sleep-wake cycle, New York: Raven Press; 1984, p. 129–57.

[5] Daan S, Beersma DGM, Borbely AA. Timing of human sleep: recovery process gated by a circadian pacemaker. Am J Physiol 1984;246. https://doi.org/10.1152/AJPREGU.1984.246.2.R161.

[6] Alexander Borbély. The two-process model of sleep regulation: Beginnings and outlook. J Sleep Res 2022:1–8.

[7] Borbély AA, Daan S, Wirz-Justice A, Deboer T. The two-process model of sleep regulation: a reappraisal. J Sleep Res 2016;25:131–43. https://doi.org/10.1111/JSR.12371.

[8] Booth V, Diniz Behn CG. Physiologically-based modeling of sleep-wake regulatory networks. Math Biosci 2014;250:54–68. https://doi.org/10.1016/J.MBS.2014.01.012.

[9] Dijk DJ, Kronauer RE. Commentary: models of sleep regulation: successes and continuing challenges. J Biol Rhythms 1999;14:571–5. https://doi.org/10.1177/074873099129000902.

[10] Beckwith EJ, French AS. Sleep in Drosophila and Its Context. Front Physiol 2019;10. https://doi.org/10.3389/fphys.2019.01167.

[11] Deboer T. Sleep homeostasis and the circadian clock: Do the circadian pacemaker and the sleep homeostat influence each other's functioning? Neurobiol Sleep Circadian Rhythms 2018;5. https://doi.org/10.1016/j.nbscr.2018.02.003.

[12] Hendricks JC, Finn SM, Panckeri KA, Chavkin J, Williams JA, Sehgal A, et al. Rest in Drosophila Is a Sleep-like State. Neuron 2000;25:129–38. https://doi.org/10.1016/S0896-6273(00)80877-6.

[13] Shaw PJ, Cirelli C, Greenspan RJ, Tononi G. Correlates of Sleep and Waking in Drosophila melanogaster. Science (1979) 2000;287:1834–7. https://doi.org/10.1126/SCIENCE.287.5459.1834.

[14] Shafer OT, Keene AC. The Regulation of Drosophila Sleep. Current Biology 2021;31:R38–49. https://doi.org/10.1016/J.CUB.2020.10.082.

[15] Shafer OT, Keene AC. The Regulation of Drosophila Sleep. Curr Biol 2021;31:R38–49. https://doi.org/10.1016/J.CUB.2020.10.082.

[16] Artiushin G, Sehgal A. The Drosophila circuitry of sleep–wake regulation. Curr Opin Neurobiol 2017;44. https://doi.org/10.1016/j.conb.2017.03.004.

[17] Helfrich-Förster C. Sleep in Insects. Annu Rev Entomol 2018;63. https://doi.org/10.1146/annurev-ento-020117-043201.

[18] Donlea JM, Thimgan MS, Suzuki Y, Gottschalk L, Shaw PJ. Inducing sleep by remote control facilitates memory consolidation in Drosophila. Science (1979) 2011;332. https://doi.org/10.1126/science.1202249.

[19] Liu S, Liu Q, Tabuchi M, Wu MN. Sleep drive is encoded by neural plastic changes in a dedicated circuit. Cell 2016;165. https://doi.org/10.1016/j.cell.2016.04.013.

[20] Donlea JM, Pimentel D, Talbot CB, Kempf A, Omoto JJ, Hartenstein V, et al. Recurrent Circuitry for Balancing Sleep Need and Sleep. Neuron 2018;97. https://doi.org/10.1016/j.neuron.2017.12.016.

[21] Pimentel D, Donlea JM, Talbot CB, Song SM, Thurston AJF, Miesenböck G. Operation of a homeostatic sleep switch. Nature 2016;536. https://doi.org/10.1038/nature19055.

[22] Liu Q, Liu S, Kodama L, Driscoll MR, Wu MN. Two dopaminergic neurons signal to the dorsal fan-shaped body to promote wakefulness in Drosophila. Current Biology 2012;22. https://doi.org/10.1016/j.cub.2012.09.008.

[23] Donlea JM, Pimentel D, Miesenböck G. Neuronal machinery of sleep homeostasis in Drosophila. Neuron 2014;81. https://doi.org/10.1016/j.neuron.2013.12.013.

[24] Kempf A, Song SM, Talbot CB, Miesenböck G. A potassium channel β-subunit couples mitochondrial electron transport to sleep. Nature 2019;568. https://doi.org/10.1038/s41586-019-1034-5.

[25] Aso Y, Sitaraman D, Ichinose T, Kaun KR, Vogt K, Belliart-Guérin G, et al. Mushroom body output neurons encode valence and guide memory-based action selection in Drosophila. Elife 2014;3. https://doi.org/10.7554/eLife.04580.

[26] Joiner WJ, Crocker A, White BH, Sehgal A. Sleep in Drosophila is regulated by adult mushroom bodies. Nature 2006;441. https://doi.org/10.1038/nature04811.

[27] Blum ID, Keleş MF, Baz ES, Han E, Park K, Luu S, et al. Astroglial Calcium Signaling Encodes Sleep Need in Drosophila. Current Biology 2021;31. https://doi.org/10.1016/j.cub.2020.10.012.

[28] Liu S, Lamaze A, Liu Q, Tabuchi M, Yang Y, Fowler M, et al. WIDE AWAKE mediates the circadian timing of sleep onset. Neuron 2014;82:151–66. https://doi.org/10.1016/j.neuron.2014.01.040.

[29] Blum ID, Bell B, Wu MN. Time for Bed: Genetic Mechanisms Mediating the Circadian Regulation of Sleep. Trends in Genetics 2018;34. https://doi.org/10.1016/j.tig.2018.01.001.

[30] Shaw P, Cirelli C, Greenspan R, Tononi G. Correlates of sleep and waking in Drosophila melanogaster. Science 2000;287:1834–7. https://doi.org/10.1126/SCIENCE.287.5459.1834.

[31] Borbély AA, Schneider D. Secrets of sleep 1986:228.

[32] Shaw PJ, Franken P. Perchance to dream: solving the mystery of sleep through genetic analysis. J Neurobiol 2003;54:179–202. https://doi.org/10.1002/NEU.10167.

[33] Stahl BA, Slocumb ME, Chaitin H, DiAngelo JR, Keene AC. Sleep-dependent modulation of metabolic rate in drosophila. Sleep 2017;40. https://doi.org/10.1093/sleep/zsx084.

[34] van Alphen B, Yap MHW, Kirszenblat L, Kottler B, van Swinderen B. A dynamic deep sleep stage in Drosophila. Journal of Neuroscience 2013;33. https://doi.org/10.1523/JNEUROSCI.0061-13.2013.

[35] Yap MHW, Grabowska MJ, Rohrscheib C, Jeans R, Troup M, Paulk AC, et al. Oscillatory brain activity in spontaneous and induced sleep stages in flies. Nat Commun 2017;8. https://doi.org/10.1038/s41467-017-02024-y.

[36] Xu X, Yang W, Tian B, Sui X, Chi W, Rao Y, et al. Quantitative investigation reveals distinct phases in Drosophila sleep. Commun Biol 2021;4. https://doi.org/10.1038/s42003-021-01883-y.

[37] Wiggin TD, Goodwin PR, Donelson NC, Liu C, Trinh K, Sanyal S, et al. Covert sleep-related biological processes are revealed by probabilistic analysis in Drosophila. Proc Natl Acad Sci U S A 2020;117. https://doi.org/10.1073/pnas.1917573117.

[38] Tainton-Heap LAL, Kirszenblat LC, Notaras ET, Grabowska MJ, Jeans R, Feng K, et al. A Paradoxical Kind of Sleep in Drosophila melanogaster. Current Biology 2021;31. https://doi.org/10.1016/j.cub.2020.10.081.

[39] Raccuglia D, Huang S, Ender A, Heim MM, Laber D, Suárez-Grimalt R, et al. Network-Specific Synchronization of Electrical Slow-Wave Oscillations Regulates Sleep Drive in Drosophila. Current Biology 2019;29. https://doi.org/10.1016/j.cub.2019.08.070.

[40] Abhilash L. phase: Analyse Biological Time-Series Data 2021.

[41] Refinetti R, Cornélissen G, Halberg F. Procedures for numerical analysis of circadian rhythms. Biol Rhythm Res 2007;38:275–325. https://doi.org/10.1080/09291010600903692.

[42] Ruf T. The Lomb-Scargle periodogram in biological rhythm research: Analysis of incomplete and unequally spaced time-series. Biol Rhythm Res 1999;30. https://doi.org/10.1076/brhm.30.2.178.1422.

[43] Brown LA, Fisk AS, Pothecary CA, Peirson SN. Telling the time with a broken clock: Quantifying circadian disruption in animal models. Biology (Basel) 2019;8. https://doi.org/10.3390/biology8010018.

[44] Tackenberg MC, Hughey JJ. The risks of using the chi-square periodogram to estimate the period of biological rhythms. PLoS Comput Biol 2021;17. https://doi.org/10.1371/JOURNAL.PCBI.1008567.

[45] Lack LC, Lushington K. The rhythms of human sleep propensity and core body temperature. J Sleep Res 1996;5:1–11. https://doi.org/10.1046/J.1365-2869.1996.00005.X.

[46] Dowse HB, Hall JC, Ringo JM. Circadian and ultradian rhythms in period mutants of Drosophila melanogaster. Behav Genet 1987;17. https://doi.org/10.1007/BF01066008.

[47] Seki Y, Tanimura T. Ultradian rhythm unmasked in the Pdf clock mutant of Drosophila. J Biosci 2014;39. https://doi.org/10.1007/s12038-014-9450-z.

[48] Leise TL. Wavelet analysis of circadian and ultradian behavioral rhythms. J Circadian Rhythms 2013;11:5. https://doi.org/10.1186/1740-3391-11-5.

[49] Brancaccio M, Edwards MD, Patton AP, Smyllie NJ, Chesham JE, Maywood ES, et al. Cell-autonomous clock of astrocytes drives circadian behavior in mammals. Science (1979) 2019;363. https://doi.org/10.1126/science.aat4104.

[50] Leise TL. Analysis of Nonstationary Time Series for Biological Rhythms Research: Http://DxDoiOrg/101177/0748730417709105 2017;32:187–94. https://doi.org/10.1177/0748730417709105.

[51] Price TS, Baggs JE, Curtis AM, Fitzgerald GA, Hogenesch JB. WAVECLOCK: wavelet analysis of circadian oscillation. Bioinformatics 2008;24:2794–5. https://doi.org/10.1093/BIOINFORMATICS/BTN521.

[52] Dowse HB, Ringo JM. Further Evidence that the Circadian Clock in Drosophila is a Population of Coupled Ultradian Oscillators. J Biol Rhythms 1987;2. https://doi.org/10.1177/074873048700200106.

[53] Tobler I, Borbély AA, Groos G. The effect of sleep deprivation on sleep in rats with suprachiasmatic lesions. Neurosci Lett 1983;42. https://doi.org/10.1016/0304-3940(83)90420-2.

[54] Wisor JP, O'Hara BF, Terao A, Selby CP, Kilduff TS, Sancar A, et al. A role of cryptochromes in sleep regulation. BMC Neurosci 2002;3. https://doi.org/10.1186/1471-2202-3-20.

[55] Larkin JE, Yokogawa T, Heller HC, Franken P, Ruby NF. Homeostatic regulation of sleep in arrhythmic Siberian hamsters. Am J Physiol Regul Integr Comp Physiol 2004;287. https://doi.org/10.1152/ajpregu.00676.2003.

[56] Trachsel L, Edgar DM, Seidel WF, Craig Heller H. Sleep homeostasis in suprachiasmatic nuclei-lesioned rats: effects of sleep deprivation and triazolam administration. Brain Res 1992;589:253–61. https://doi.org/10.1016/0006-8993(92)91284-L.

[57] Naylor E, Bergmann BM, Krauski K, Zee PC, Takahashi JS, Vitaterna MH, et al. The circadian Clock mutation alters sleep homeostasis in the mouse. Journal of Neuroscience 2000;20. https://doi.org/10.1523/jneurosci.20-21-08138.2000.

[58] Franken P, Thomason R, Craig HC, O'Hara BF. A non-circadian role for clock-genes in sleep homeostasis: A strain comparison. BMC Neurosci 2007;8. https://doi.org/10.1186/1471-2202-8-87.

[59] Laposky A, Easton A, Dugovic C, Walisser J, Bradfield C, Turek F. Deletion of the mammalian circadian clock gene BMAL1/Mop3 alters baseline sleep architecture and the response to sleep deprivation. Sleep 2005;28. https://doi.org/10.1093/sleep/28.4.395.

[60] Shaw PJ, Tortoni G, Greenspan RJ, Robinson DF. Stress response genes protect against lethal effects of sleep deprivation in Drosophila. Nature 2002;417. https://doi.org/10.1038/417287a.

[61] Shiromani PJ, Xu M, Winston EM, Shiromani SN, Gerashchenko D, Weaver DR. Sleep rhythmicity and homeostasis in mice with targeted disruption of mPeriod genes. Am J Physiol Regul Integr Comp Physiol 2004;287. https://doi.org/10.1152/ajpregu.00138.2004.

[62] Dijk DJ, Archer SN. PERIOD3, circadian phenotypes, and sleep homeostasis. Sleep Med Rev 2010;14. https://doi.org/10.1016/j.smrv.2009.07.002.

[63] Konopka RJ, Hamblen-Coyle MJ, Jamison CF, Hall JC. An Ultrashort Clock Mutation at the period Locus of Drosophila melanogaster That Reveals Some New Features of the Fly's Circadian System. J Biol Rhythms 1994;9. https://doi.org/10.1177/074873049400900303.

[64] Konopka RJ, Benzer S. Clock Mutants of Drosophila melanogaster. Proceedings of the National Academy of Sciences 1971;68:2112–6. https://doi.org/10.1073/pnas.68.9.2112.

[65] Hoofdakker R, van Den H, Bos KHN, van den Burg W. In search of a depressive sleep syndrome. In: van Praag HM, Meinardi H, editors. Brain and Sleep, Amsterdam: Bohn: 1974.

[66] Franken P, Dijk DJ, Tobler I, Borbely AA. Sleep deprivation in rats: Effects on EEG power spectra, vigilance states, and cortical temperature. Am J Physiol Regul Integr Comp Physiol 1991;261. https://doi.org/10.1152/ajpregu.1991.261.1.r198.

[67] Schlichting M, Menegazzi P, Rosbash M, Helfrich-Förster C. A Distinct Visual Pathway Mediates High-Intensity Light Adaptation of the Circadian Clock in Drosophila. The Journal of Neuroscience 2019;39:1621. https://doi.org/10.1523/JNEUROSCI.1497-18.2018.

[68] Dubowy C, Sehgal A. Circadian rhythms and sleep in Drosophila melanogaster. Genetics 2017;205. https://doi.org/10.1534/genetics.115.185157.

[69] Zar JH. Biostatistical analysis. Prentice Hall; 1999.

[70] Emery P, Stanewsky R, Helfrich-Förster C, Emery-Le M, Hall JC, Rosbash M. Drosophila CRY Is a Deep Brain Circadian Photoreceptor. Neuron 2000;26:493–504. https://doi.org/10.1016/S0896-6273(00)81181-2.

[71] Stanewsky R, Kaneko M, Emery P, Beretta B, Wager-Smith K, Kay SA, et al. The cryb Mutation Identifies Cryptochrome as a Circadian Photoreceptor in Drosophila. Cell 1998;95:681–92. https://doi.org/10.1016/S0092-8674(00)81638-4.

[72] Hunter-Ensor M, Ousley A, Sehgal A. Regulation of the Drosophila protein timeless suggests a mechanism for resetting the circadian clock by light. Cell 1996;84. https://doi.org/10.1016/S0092-8674(00)81046-6.

[73] Leise TL, Harrington ME. Wavelet-based time series analysis of Circadian rhythms. J Biol Rhythms 2011;26. https://doi.org/10.1177/0748730411416330.

[74] Riggle JP, Kay LM, Onishi KG, Falk DT, Smarr BL, Zucker I, et al. Modified Wavelet Analyses Permit Quantification of Dynamic Interactions Between Ultradian and Circadian Rhythms. J Biol Rhythms 2022;37:631–54. https://doi.org/10.1177/07487304221128652.

[75] Persons JL, Abhilash L, Lopatkin AJ, Roelofs A, Bell E v, Fernandez MP, et al. PHASE: An Open-Source Program for the Analysis of DrosophilaPhase, Activity, and Sleep Under Entrainment. J Biol Rhythms 2022;37:455–67. https://doi.org/10.1177/07487304221093114.

[76] Tobler I, Stalder J. Rest in the scorpion - a sleep-like state? Journal of Comparative Physiology A 1988;163. https://doi.org/10.1007/BF00612431.

[77] Vorster APA, Krishnan HC, Cirelli C, Lyons LC. Characterization of sleep in Aplysia californica. Sleep 2014;37. https://doi.org/10.5665/sleep.3992.

[78] Ramón F, Hernández-Falcón J, Nguyen B, Bullock TH. Slow wave sleep in crayfish. Proc Natl Acad Sci U S A 2004;101. https://doi.org/10.1073/pnas.0402015101.

[79] Ajayi OM, Marlman JM, Gleitz LA, Smith ES, Piller BD, Krupa JA, et al. Behavioral and postural analyses establish sleep-like states for mosquitoes that can impact host landing and blood feeding. Journal of Experimental Biology 2022;225:jeb244032. https://doi.org/10.1242/jeb.244032.

[80] Kaiser W, Steiner-Kaiser J. Sleep Research on Honeybees: Neurophysiology and Behavior. Neurobiology and Behavior of Honeybees, 1987. https://doi.org/10.1007/978-3-642-71496-2_10.

[81] Kanaya HJ, Park S, Kim JH, Kusumi J, Krenenou S, Sawatari E, et al. A sleep-like state in Hydra unravels conserved sleep mechanisms during the evolutionary development of the central nervous system. Sci Adv 2020;6. https://doi.org/10.1126/sciadv.abb9415.

[82] Prabhakaran PM, Sheeba V. Sympatric drosophilid species melanogaster and ananassae differ in temporal patterns of activity. J Biol Rhythms 2012;27. https://doi.org/10.1177/0748730412458661.

[83] Jaggard J, Robinson BG, Stahl BA, Oh I, Masek P, Yoshizawa M, et al. The lateral line confers evolutionarily derived sleep loss in the Mexican cavefish. Journal of Experimental Biology 2017;220. https://doi.org/10.1242/jeb.145128.

[84] Brown EB, Torres J, Bennick RA, Rozzo V, Kerbs A, DiAngelo JR, et al. Variation in sleep and metabolic function is associated with latitude and average temperature in Drosophila melanogaster. Ecol Evol 2018;8. https://doi.org/10.1002/ece3.3963.

[85] Achermann P, Borbély AA. Simulation of Human Sleep: Ultradian Dynamics of Electroencephalographic Slow-Wave Activity. J Biol Rhythms 1990;5. https://doi.org/10.1177/074873049000500206.

[86] ACHERMANN P, BORBÉLY AA. Combining different models of sleep regulation. J Sleep Res 1992;1. https://doi.org/10.1111/j.1365-2869.1992.tb00028.x.

[87] Achermann P, Dijk DJ, Brunner DP, Borbély AA. A model of human sleep homeostasis based on EEG slow-wave activity: Quantitative comparison of data and simulations. Brain Res Bull 1993;31. https://doi.org/10.1016/0361-9230(93)90016-5.

[88] Mistlberger RE, Bergmann BM, Waldenar W, Rechtschaffen A. Recovery sleep following sleep deprivation in intact and suprachiasmatic nuclei-lesioned rats. Sleep 1983;6. https://doi.org/10.1093/sleep/6.3.217.

[89] Dowse HB, Ringo JM. Do Ultradian Oscillators Underlie the Circadian Clock in Drosophila? Ultradian Rhythms in Life Processes, 1992. https://doi.org/10.1007/978-1-4471-1969-2_6.

[90] Dijk DJ, Beersma DGM, Daan S. EEG Power Density during Nap Sleep: Reflection of an Hourglass Measuring the Duration of Prior Wakefulness. J Biol Rhythms 1987;2. https://doi.org/10.1177/074873048700200304.

[91] Marrus SB, Zeng H, Rosbash M. Effect of constant light and circadian entrainment of perS flies: evidence for light-mediated delay of the negative feedback loop in Drosophila. EMBO J 1996;15:6877. https://doi.org/10.1002/j.1460-2075.1996.tb01080.x.

[92] Li Y, Shan Y, Kilaru G, Berto S, Wang GZ, Cox KH, et al. Epigenetic inheritance of circadian period in clonal cells. Elife 2020;9. https://doi.org/10.7554/eLife.54186.

[93] Nikhil KL, Korge S, Kramer A. Heritable gene expression variability and stochasticity govern clonal heterogeneity in circadian period. PLoS Biol 2020;18. https://doi.org/10.1371/JOURNAL.PBIO.3000792.

[94] Viola AU, Archer SN, James LMM, Groeger JA, Lo JCY, Skene DJ, et al. PER3 Polymorphism Predicts Sleep Structure and Waking Performance. Current Biology 2007;17. https://doi.org/10.1016/j.cub.2007.01.073.

[95] Huber R, Deboer T, Tobler I. Effects of sleep deprivation on sleep and sleep EEG in three mouse strains: Empirical data and simulations. Brain Res 2000;857. https://doi.org/10.1016/S0006-8993(99)02248-9.

[96] Franken P, Tobler I, Borbély AA. Sleep homeostasis in the rat: Simulation of the time course of EEG slow-wave activity. Neurosci Lett 1991;130. https://doi.org/10.1016/0304-3940(91)90382-4.

[97] Schwartz WJ, Zimmerman P. Circadian timekeeping in BALB/c and C57BL/6 inbred mouse strains. Journal of Neuroscience 1990;10. https://doi.org/10.1523/jneurosci.10-11-03685.1990.

[98] Czeisler CA, Duffy JF, Shanahan TL, Brown EN, Mitchell JF, Rimmer DW, et al. Stability, precision, and near-24-hour period of the human circadian pacemaker. Science (1979) 1999;284. https://doi.org/10.1126/science.284.5423.2177.

[99] Abhilash L, Shafer OT. Parametric effects of light acting via multiple photoreceptor types contribute significantly to circadian entrainment in Drosophila melanogaster. BioRxiv 2022:2022.03.02.482722. https://doi.org/10.1101/2022.03.02.482722.

[100] Liang X, Holy TE, Taghert PH. Synchronous drosophila circadian pacemakers display nonsynchronous Ca2+ rhythms in vivo. Science (1979) 2016;351. https://doi.org/10.1126/science.aad3997.

[101] Lamaze A, Krätschmer P, Chen KF, Lowe S, Jepson JEC. A Wake-Promoting Circadian Output Circuit in Drosophila. Current Biology 2018;28. https://doi.org/10.1016/j.cub.2018.07.024.

[102] Kunst M, Hughes ME, Raccuglia D, Felix M, Li M, Barnett G, et al. Calcitonin gene-related peptide neurons mediate sleep-specific circadian output in Drosophila. Current Biology 2014;24. https://doi.org/10.1016/j.cub.2014.09.077.

[103] Guo F, Holla M, Díaz MM, Rosbash M. A Circadian Output Circuit Controls Sleep-Wake Arousal in Drosophila. Neuron 2018;100. https://doi.org/10.1016/j.neuron.2018.09.002.

[104] Guo F, Yu J, Jung HJ, Abruzzi KC, Luo W, Griffith LC, et al. Circadian neuron feedback controls the Drosophila sleep-activity profile. Nature 2016;536. https://doi.org/10.1038/nature19097.

[105] Barber AF, Erion R, Holmes TC, Sehgal A. Circadian and feeding cues integrate to drive rhythms of physiology in Drosophila insulin-producing cells. Genes Dev 2016;30. https://doi.org/10.1101/gad.288258.116.
[106] Roesch A, Schmidbauer H. WaveletComp: Computational Wavelet Analysis 2018.
[107] Aldrich E. wavelets: Functions for Computing Wavelet Filters, Wavelet Transforms and Multiresolution Analyses 2020.
[108] Kohl M. MKinfer: Inferential Statistics 2022.
[109] Geissmann Q, Beckwith EJ, Gilestro GF. Most sleep does not serve a vital function: Evidence from Drosophila melanogaster. Sci Adv 2019;5. https://doi.org/10.1126/SCIADV.AAU9253.
[110] R Core Team. R: A Language and Environment for Statistical Computing 2019.
[111] Ram K, Wickham H. wesanderson: A Wes Anderson Palette Generator 2018.

Figure Legends

Figure 1: Circadian analysis of *Drosophila* sleep. (A) A schematic of the two-process model that leads to one episode of sleep/cycle. (B) Somnograms (left) and actograms (right) of *Canton-S* (*CS*; top), w^{1118} (middle) and *yw* (bottom) flies under light/dark 12:12 (LD12:12) cycles and constant darkness (DD). Gray shaded regions indicate the dark phase of the LD cycle. Representative Chi-square periodograms of sleep time-series (C) under LD12:12 (top) and DD (bottom), and of locomotor activity time-series (D) under LD12:12 (top) and DD (bottom) of the three genotypes of flies. The red lines indicate the Chi-square significance line at $\alpha = 0.05$. Height of peaks of the black lines indicate the strength of that periodicity in the time-series. Gray shaded regions indicate the dark phase of the LD cycle. (E) Frequency distributions of percentage time spent sleeping/24-h cycle in the three genotypes under LD12:12.

Figure 2: Building a *Drosophila* two-process model of sleep regulation. (A) Schematic of the two-process model that leads to two episodes of sleep/cycle taken from Daan et al. 1984 [5]. (B) Heatmap summarizing the nature of sleep rhythms within the build-up and decay of sleep pressure parameter space. (C) Heatmap showing the sum of squared differences (SSD) between model prediction and empirical values in the same parameter space for the value combinations producing bimodal rhythms. The red arrowhead marks the parameters that yield minimum SSD, revealing the values that describe fly sleep best. Both panels (B) and (C) share the same *y*-axis. (D) The two-process model with best-fitting parameters. (E) the percentage of time spent sleeping/24-cycle in the three genotypes compared with the predicted value from the model plotted in (D).

Figure 3: Ultradian periodicities are a predictable consequence of a functioning S-process under a dysfunctional C-process. (A) A two-process model with the best-fitting homeostatic parameters and a circadian clock speed of 24-h (top). Also shown is the somnogram of simulated sleep data produced by this model (bottom). (B) The same model as in panel (A) but with flat, non-oscillating thresholds to model sleep regulation in a loss-of-function clock mutant (top), and the somnogram it produced (bottom). (C) Four representative continuous wavelet transform (CWT) spectrograms for *Canton-S* (*CS*; C) and (D) one each for per^{01}, tim^{01}, clk^{JRK} and cyc^{01}. The color bars against each spectrogram are representative of local rhythmic power. Note: the *y*-axes on the spectrograms are on a logarithmic scale. (E) Normalized (to maximum count) frequency distributions of period values detected by CWT for each of the five aforementioned fly genotypes. Each gray trace is the histogram of detected periods for a single fly. The red trace in each plot is the average histogram across all flies. The *x*- and *y*-axis are common for all five plots.

Figure 4: The model predicts regions of unstable sleep rhythms across a range of free-running periods. (A) Schematic representation of the simulation based on which predictions were made. (B) Predicted power of sleep rhythms under conditions of varying C-process period values. Red shaded regions mark zones of low power. Also shown are simulated somnograms. (C) Power of sleep rhythms and (D) time spent sleeping/circadian minute for flies with different free-running periods, generated through combinations of five *period* alleles (see Methods).

Figure 5: Empirical estimates of power and amount of sleep modestly match predictions from the two-process model. (A) Median power of sleep rhythms and (B) time spent sleeping/circadian minute across the entire range of free-running periods overlayed with the

predictions of the two-process model when only the free-running period was altered in the model. (C) Schematic representation of the simulation routine to estimate the best fitting S-process parameter for each individual fly. (D) Median power of sleep rhythms and (E) time spent sleeping/circadian minute across the entire range of free-running periods overlayed with predictions of the best-fit two-process model where homeostatic sleep pressure parameters covaried with free-running period.

Figure 6: Allowing homeostatic parameters to change with free-running periods reveal a complex inter-dependence between the S- and C-processes. (A) The relationship between build-up of sleep pressure and free-running periods, and (B) decay of sleep pressure and free-running periods used in the altered model. The red lines overlaying the boxplots are median values and the dark green line is a loess regression (locally weighted polynomial regression) smoothed fit. Higher values on the *y*-axis of the build-up of sleep pressure panel and lower values on the *y*-axis of the decay of sleep pressure panel indicate steeper rise and fall of sleep pressure in the model, respectively. Panels (A) and (B) share the same *x*-axis. Also shown are the regions along the *x*-axis corresponding to the free-running periods of males bearing the four rhythmic *period* alleles used in our study (see also Table 2). Boxplots sharing the same letters of the alphabet are not statistically significantly different from each other.

Figure 7: Long bout sleep reflects the S-process mediated sleep better than the standard definition of fly sleep. (A) Scatter plots of the normalized time spent sleeping/circadian minute across different free-running periods for different inactivity duration-based definitions of sleep overlayed with the amounts of sleep measured using standard definition of sleep and the amounts

predicted by the model. (B) The correlation coefficients from Pearson's product-moment correlations between model predictions of normalized time spent sleeping/circadian minute and for different inactivity duration-based definitions of sleep. (C) Representative continuous wavelet transforms (CWT) spectrograms for *CS* and per^{01} flies that were recorded under constant darkness (DD) using two different inactivity duration criteria for sleep (see Materials and Methods). The color bars above each spectrogram are representative of local rhythmic power. Note: the *y*-axes on the spectrograms are on a logarithmic scale. (D) Normalized (to maximum count) frequency distributions of detected periodicities across all flies for both genotypes for the two different inactivity duration-based definitions of sleep. The *y*-axis is shared by both plots. Note how biasing the definition of sleep towards long bouts of inactivity does not drastically change the distribution in wildtype flies.

Figure 8: Long bout sleep has distinct temporal organization under entrained and free-running conditions. (A) Sleep time-series of *Canton-S* (*CS*) flies under three days of LD12:12 and four days of constant darkness (DD) for different definitions of sleep (see Materials and Methods). Dark gray shaded regions in the plots indicate the dark phase of LD cycles and subjective dark phases under DD (i.e., when darkness would have occurred had the previous LD cycle continued). The light gray shaded regions indicate the subjective day phases under DD. (B) A time-series of *Canton-S* (*CS*) sleep under fifteen days of constant darkness reveals a drastic reduction in long bout sleep during the subjective day (shaded rectangles) as compared to almost no reduction in subjective night-time sleep (orange arrows).

Figure 9: Independent tests confirm the relationship between free-running period and the rates of change of sleep homeostat. (A) Schematic representation of the predictions if short period flies have altered homeostatic parameters. (B) Time-series of long bout sleep of both genotypes under continuous white light for 15 cycles. Discrete wavelet transform based estimate of index-wise concentration of spectral variance in (C) *CS* and (D) per^S flies (also see Methods). Shown are mean estimates of percentage of variance±SEM. Note the three period bands that comprise maximal spectral energy. (E) Ultradian periods (mean±SEM) for the two genotypes under LL as estimated from the continuous wavelet transforms (Results based on one-tailed bootstrapped Welch two-sample *t*-tests – τ_s: $t_{30.72} = 2.49$, $p = 0.004$; τ_m: $t_{29.46} = 0.57$, $p = 0.30$; τ_l: $t_{35.58} = -1.19$, $p = 0.88$). (F) Boxplots of total sleep over 15 cycles ($W = 860$; $p = 4.18e\text{-}07$) and (G) of total number of long bout sleep episodes over 15 cycles ($W = 264.5$; $p = 0.0005$) show significant differences in the direction predicted by the model. Statistical comparisons were made using the one-tailed Wilcoxon's test. * < 0.05, ** < 0.01, *** < 0.001, **** < 0.0001, and N.S. (Not Significant).

Figure 10: Utility of the two-process model in generating testable predictions. (A) Predicted roles played by the rising and falling phases of the thresholds in regulating the timing and maintenance of sleep, in the context of the two-process model. Hypothetical relationships between Ca^{2+} levels in circadian clock neurons, the two-process model, and sleep behavior. Data for the Ca^{2+} levels were extracted from Liang et al., 2016 and smoothed using custom R scripts. Light gray shaded regions represent the subjective day phase, and the dark gray shaded regions represent the subjective night phase of one circadian cycle. Note how the peak of LNd Ca^{2+} maps onto the rising phase of the threshold oscillations and the Ca^{2+} peaks of DNs map onto the falling phase of

the thresholds of the two-process model. (B) A schematic representation of the effect of activation of DN-1s on sleep previously reported by others. Exciting DN-1ps is predicted to produce an earlier fall and prolonged suppression of the sleep threshold oscillations (dotted black lines). As a consequence of the earlier falling of the thresholds, the sleep pressure takes longer to hit the lower threshold (dotted red line) and therefore there is an increase in day-time sleep (dotted blue bounded boxes) as was observed in two previously reported studies (bottom panel). The plots in the bottom panel are redrawn from Guo et al. (2016) [104] and Kunst et al. (2014) [102]. Green lines represent sleep in the DN-1p activated flies and the black lines represent unmanipulated controls. This manipulation also leads to an earlier termination of nighttime sleep as was reported by Kunst et al., (2014) [102]. (C) Simulated C-process changes under situations of (i) complete loss of increases in thresholds, (ii) reduced increases, (iii) unchanged, (iv) reduced decreases in thresholds, and (v) complete loss of decreases. Solid black lines indicate the manipulated sleep thresholds, and the dashed black lines represent normal thresholds. The red line in all cases represents process-S. In bottom panels, black bars indicate sleep bouts and sleep are plotted as somnograms. It is Important to note that our specific quantitative prediction are produced by the best-fit two process model of fly sleep developed here and are not extrapolated from the original human two-process model.

Suppl. Figure 1: Sketch of the algorithm used for generating a two-process model for fly sleep. Step sizes for the sleep pressure parameters were set at 0.005.

Suppl. Figure 2: Individual timeseries of *per*^{01} flies under constant darkness. The red dotted lines demarcate days. Note the pervasive presence of ultradian rhythms in sleep with variable periodicities.

Suppl. Figure 3: Sketch of the algorithm used for generating predictions from a two-process model with different free-running periods of the C-process.

Suppl. Figure 4: (A) Median power of locomotor activity and sleep rhythms for flies with different free-running periods. (B) Median power of beam crossing rhythms across the entire range of free-running periods overlayed with the sleep rhythm predictions of the two-process model when only the free-running period was altered in the model.

Suppl. Figure 5: Median power of sleep rhythms across the entire range of free-running periods using the Chi-squared and Lomb-Scargle periodograms to highlight the fact that the relationship between free-running period and power of sleep rhythms is largely independent of the method chosen to estimate power of sleep rhythms. Error bars are SEM across two replicate experimental runs.

Suppl. Figure 6: Sketch of the algorithm used for generating predictions from a two-process model with different free-running periods of the C-process when the S-process parameters were also allowed to change. Step sizes for the sleep pressure parameters were set at 0.05.

Suppl. Figure 7: Estimations of the percentage of time spent sleeping/24-h day in a wide range of animal species (also see Suppl. Table 2).

Suppl. Figure 8: A schematic representation of the effect of the inhibition of synaptic transmission from the DN-1ps on sleep. We assume that inhibiting synaptic transmission of the DN-1ps will mimic the inhibition of DN-1p firing. As a consequence, reduced DN-1p output during the day (dotted green line), the sleep thresholds of the two-process model will not fall throughout the night and would remain high (black dotted lines). Such a manipulation is predicted to lead to an altered pattern of sleep pressure changes (dotted red line) that would result in the reduction and fragmentation of sleep (dotted blue bounded boxes). Such effects of inhibiting synaptic transmission in the DN-1ps were reported previously (bottom panel; Guo et al., 2016). The schematic of behavioral sleep data is redrawn from Guo et al. (2016) – green line represents the experimental flies and black line represents control flies.

Suppl. Table 1: Adjusted power values (mean±SEM) of *Canton-S* (*CS*), w^{1118} and *yw* flies from Lomb-Scargle periodogram analyses on sleep and locomotor activity time-series under LD and DD conditions in the circadian range (between 16- to 32-h). Also reported are the differences in power values between sleep and locomotor activity powers for each genotype. Sample sizes are provided in parentheses.

Suppl. Table 2: Percentage of time spent sleeping/24-h day in a range of animal species. Animals are arranged in descending order of % time spent sleeping. Data were compiled from the following sources: Cambell and Tobler, 1984; Brown et al., 2018; Ajayi et al., 2022; Prabhakaran and

Sheeba, 2012; Tobler and Stalder, 1988; Ramón et al., 2004; Vorster et al., 2014; Kanaya et al., 2020; Kaiser and Kaiser, 1987; Jaggard et al., 2017.

Tables

Table 1: Adjusted power values (mean±SEM) of *Canton-S* (*CS*), w^{1118} and *yw* flies from Chi-squared periodogram analyses on sleep and locomotor activity time-series under LD and DD conditions in the circadian range (between 16- to 32-h). Also reported are the differences in power values between sleep and locomotor activity powers for each genotype. Sample sizes are provided in parentheses.

	CS		***w^{1118}***		***yw***	
	LD12:12	**DD**	**LD12:12**	**DD**	**LD12:12**	**DD**
Sleep	4006.7 ± 163.0 (32)	2119.6 ± 242.1 (31)	3964.3 ± 138.1 (31)	3107.3 ± 200.7 (31)	3022.8 ± 211.1 (31)	1613.0 ± 140.5 (28)
Locomotor activity	1345.3 ± 180.5 (32)	503.8 ± 89.3 (28)	2657.2 ± 125.6 (31)	1200.2 ± 110.1 (31)	638.8 ± 120.7 (30)	296.2 ± 60.7 (27)
Δ Power	2661.4	1615.8	1307.1	1907.2	2384.0	1316.8

Table 2: Median free-running periods of sleep rhythms under constant darkness averaged across two-replicate runs. The values for male (top, blue) and female (bottom, red) progeny from each cross are reported. Outcomes of any cross that had fewer than 12 flies pooled from both replicate runs have not been reported in this table. Sample sizes are provided in parentheses.

Paternal genotype	Maternal genotype: per^T	per^S	per^+	per^L	per^{01}
per^T	♂: 15.25 (44) ♀: 17.75 (38)	♂: 19.75 (30) ♀: 18.50 (24)	♂: 24.25 (63) ♀: 20.50 (55)	♂: 28.75 (62) ♀: 21.75 (55)	♂: NA ♀: 19.75 (60)
per^S	♂: 17.00 (63) ♀: 19.25 (59)	♂: 21.00 (34) ♀: 20.38 (12)	♂: 24.25 (59) ♀: 22.00 (53)	♂: 28.25 (60) ♀: 23.50 (62)	♂: NA ♀: 21.50 (56)
per^+	♂: 16.25 (51) ♀: 20.75 (59)	♂: 19.63 (60) ♀: 22.00 (62)	♂: 23.50 (47) ♀: 24.00 (57)	♂: 27.50 (59) ♀: 24.75 (63)	♂: NA ♀: 25.00 (63)
per^L	♂: 16.50 (30) ♀: 22.00 (31)	♂: 20.00 (61) ♀: 23.00 (55)	♂: 24.00 (59) ♀: 24.50 (63)	♂: 27.75 (42) ♀: 27.50 (53)	♂: NA ♀: 29.75 (55)
per^{01}	♂: NA ♀: NA	♂: 20.00 (29) ♀: 21.50 (28)	♂: 24.25 (47) ♀: 25.00 (57)	♂: 28.50 (60) ♀: 29.50 (55)	♂: NA ♀: NA

Table 3: Median Chi-squared periodogram power of sleep rhythms under constant darkness averaged across two-replicate runs. The values for male (top, blue) and female (bottom, red) progeny from each cross are reported. Outcomes of any cross that had fewer than 12 flies pooled from the replicate runs have not been reported in this table. Sample sizes are provided in parentheses.

Paternal genotype \ Maternal genotype	per^T	per^S	per^+	per^L	per^{01}
per^T	♂: 33.0 (44) ♀: 33.6 (38)	♂: 187.5 (30) ♀: 143.9 (24)	♂: 136.1 (63) ♀: 79.5 (55)	♂: 135.5 (62) ♀: 98.4 (55)	♂: NA ♀: 119.4 (60)
per^S	♂: 98.0 (63) ♀: 110.7 (59)	♂: 109.7 (34) ♀: 40.7 (12)	♂: 95.9 (59) ♀: 105.1 (53)	♂: 137.5 (60) ♀: 70.8 (62)	♂: NA ♀: 103.3 (56)
per^+	♂: 51.5 (51) ♀: 76.4 (59)	♂: 161.0 (60) ♀: 117.0 (62)	♂: 79.4 (47) ♀: 92.6 (57)	♂: 64.9 (59) ♀: 118.0 (63)	♂: NA ♀: 130.3 (63)
per^L	♂: 93.7 (30) ♀: 108.4 (31)	♂: 81.1 (61) ♀: 55.5 (55)	♂: 53.9 (59) ♀: 134.0 (63)	♂: 72.0 (42) ♀: 85.4 (53)	♂: NA ♀: 92.8 (55)
per^{01}	♂: NA ♀: NA	♂: 114.6 (29) ♀: 114.4 (28)	♂: 32.7 (47) ♀: 102.4 (57)	♂: 56.1 (60) ♀: 72.7 (55)	♂: NA ♀: NA

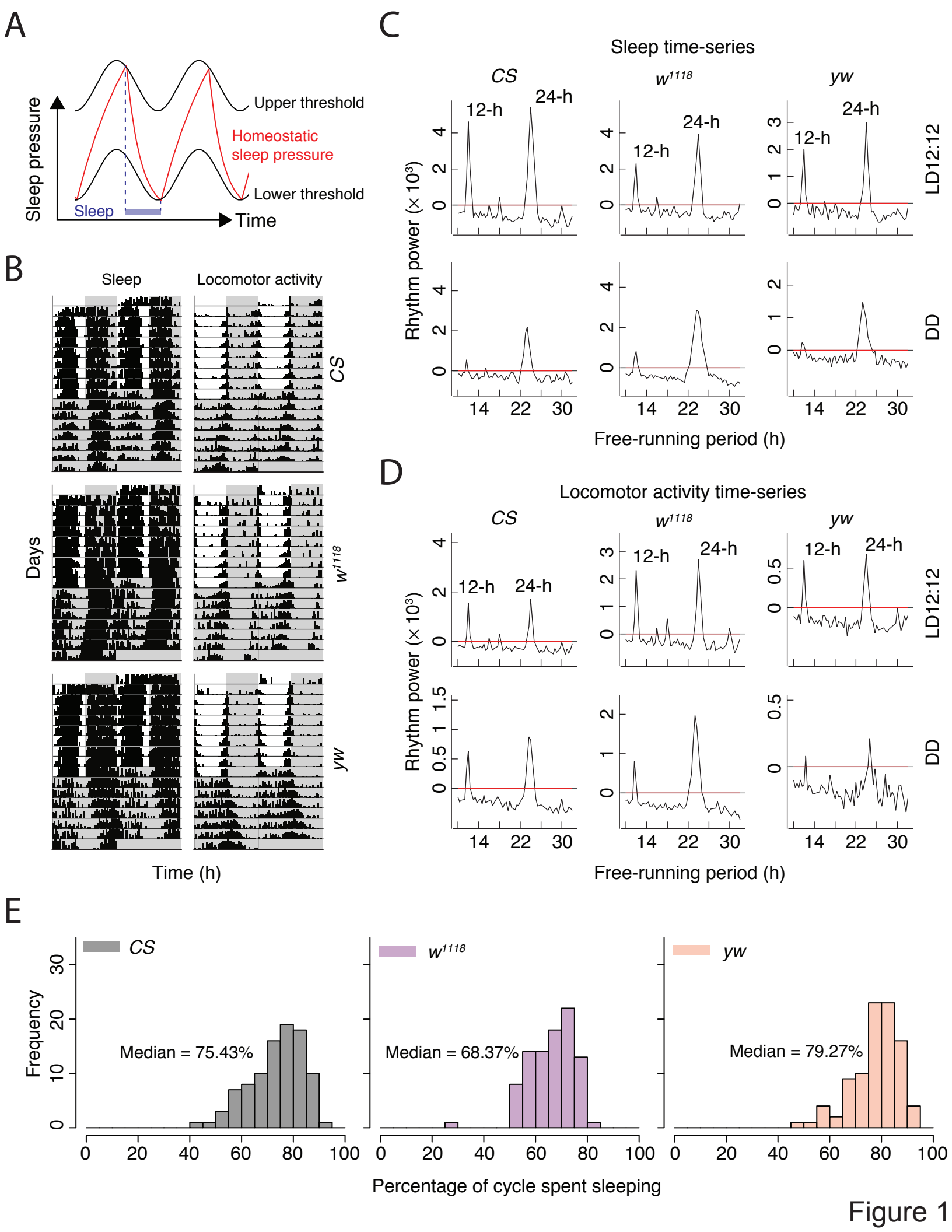
A
Sleep pressure
Upper threshold
Homeostatic sleep pressure
Lower threshold
Sleep
Time
B
Sleep
Locomotor activity
CS
w1118
yw
Days
Time (h)
C
Sleep time-series
CS
w1118
yw
12-h
24-h
LD12:12
DD
Rhythm power (× 10³)
Free-running period (h)
D
Locomotor activity time-series
CS
w1118
yw
12-h
24-h
LD12:12
DD
Rhythm power (× 10³)
Free-running period (h)
E
CS
w1118
yw
Frequency
Median = 75.43%
Median = 68.37%
Median = 79.27%
Percentage of cycle spent sleeping

Figure 1

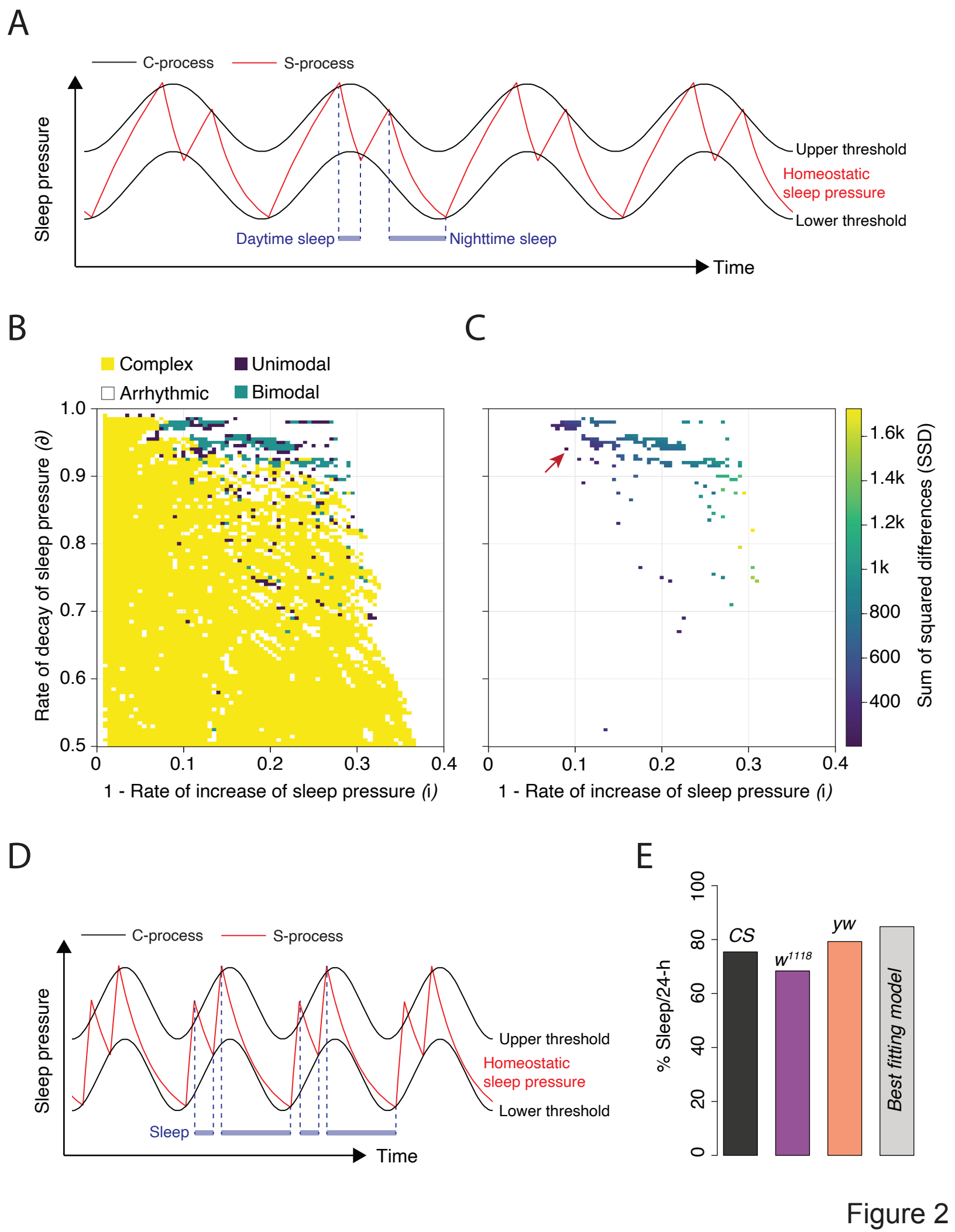
A
C-process
S-process
Sleep pressure
Upper threshold
Homeostatic sleep pressure
Lower threshold
Daytime sleep
Nighttime sleep
Time
B
Complex
Unimodal
Arrhythmic
Bimodal
Rate of decay of sleep pressure (∂)
1 - Rate of increase of sleep pressure (ı)
C
Sum of squared differences (SSD)
1.6k
1.4k
1.2k
1k
800
600
400
D
C-process
S-process
Sleep pressure
Upper threshold
Homeostatic sleep pressure
Lower threshold
Sleep
Time
E
% Sleep/24-h
CS
w1118
yw
Best fitting model

Figure 2

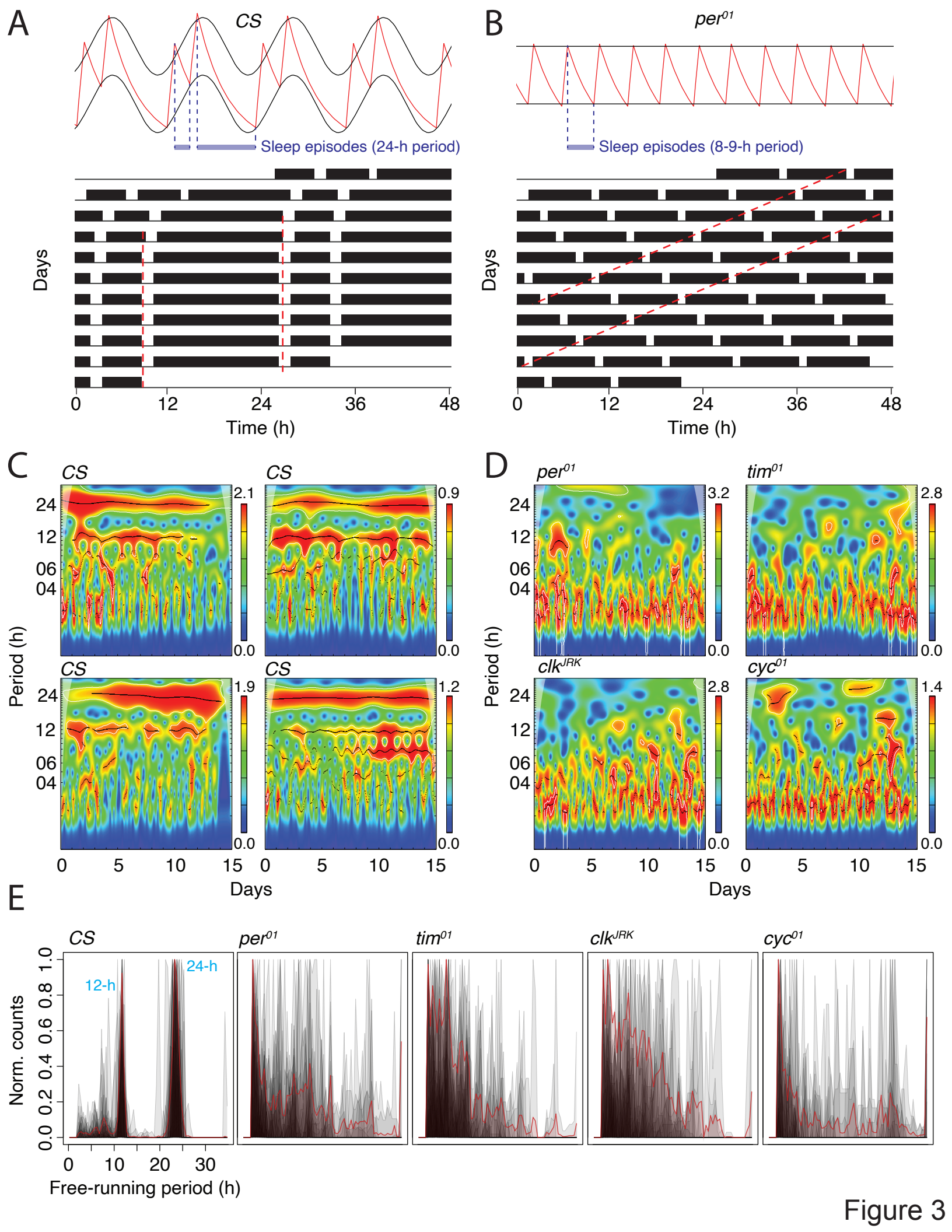
A
CS
Sleep episodes (24-h period)
Days
0
12
24
36
48
Time (h)
B
per01
Sleep episodes (8-9-h period)
Days
0
12
24
36
48
Time (h)
C
CS
CS
CS
CS
Period (h)
24
12
06
04
2.1
0.9
1.9
1.2
0.0
0
5
10
15
Days
D
per01
tim01
clkJRK
cyc01
Period (h)
24
12
06
04
3.2
2.8
2.8
1.4
0.0
0
5
10
15
Days
E
CS
per01
tim01
clkJRK
cyc01
12-h
24-h
Norm. counts
0.0
0.2
0.4
0.6
0.8
1.0
0
10
20
30
Free-running period (h)

Figure 3

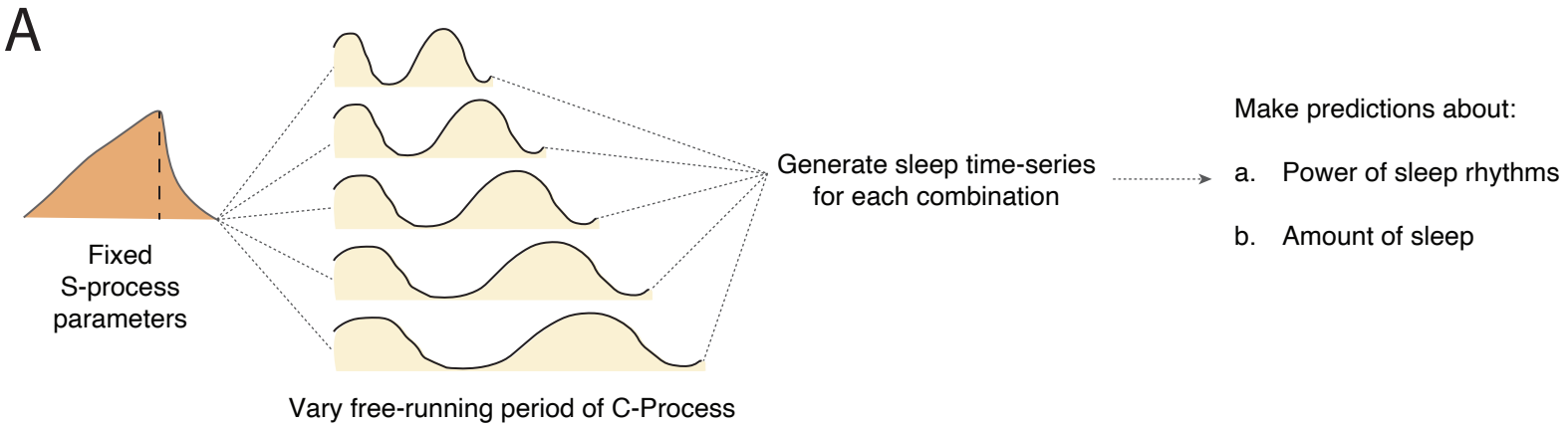
A
Fixed
S-process
parameters
Vary free-running period of C-Process
Generate sleep time-series
for each combination
Make predictions about:
a. Power of sleep rhythms
b. Amount of sleep

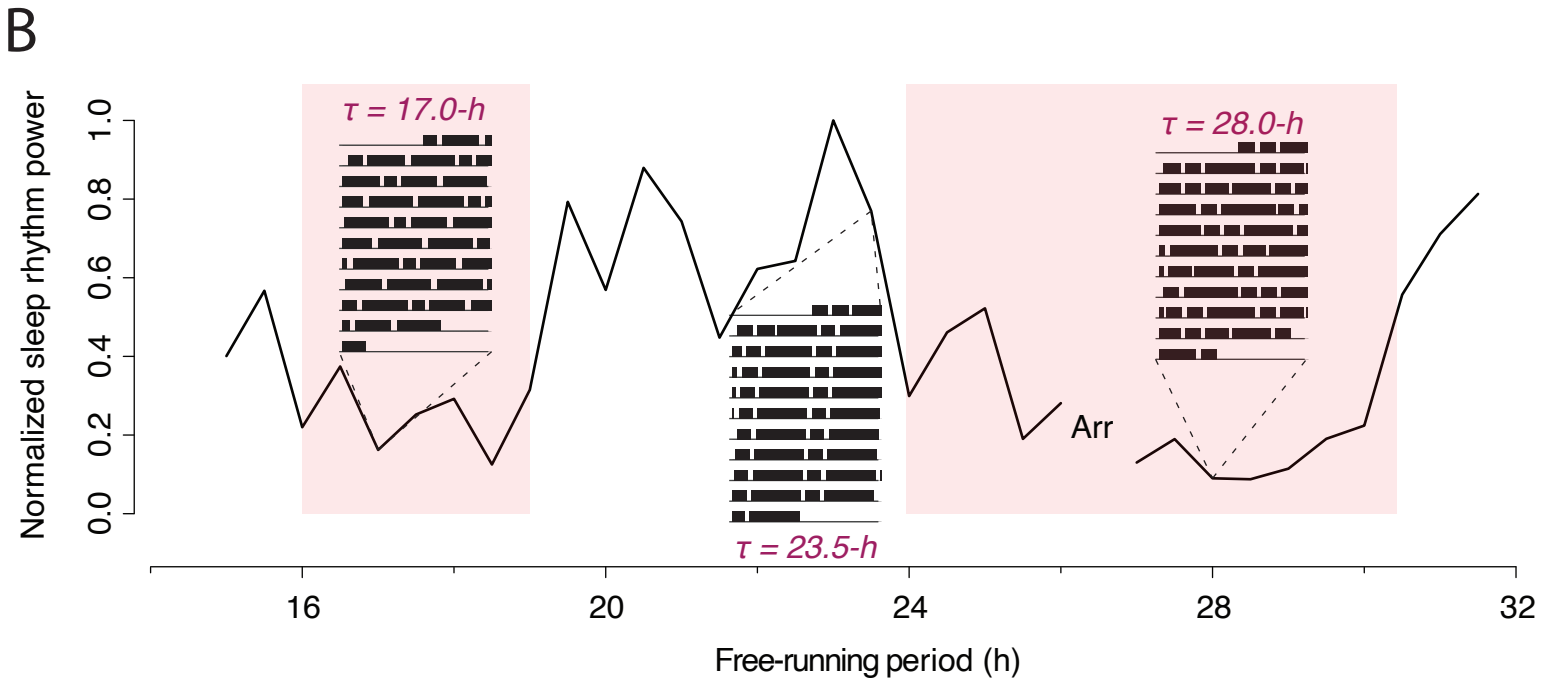
B
Normalized sleep rhythm power
0.0
0.2
0.4
0.6
0.8
1.0
τ = 17.0-h
τ = 23.5-h
τ = 28.0-h
Arr
16
20
24
28
32
Free-running period (h)

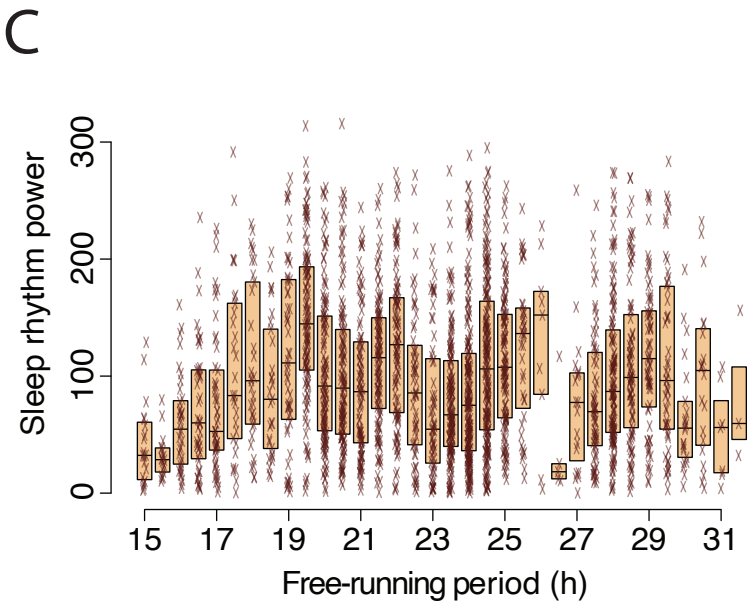
C
Sleep rhythm power
0
100
200
300
15
17
19
21
23
25
27
29
31
Free-running period (h)

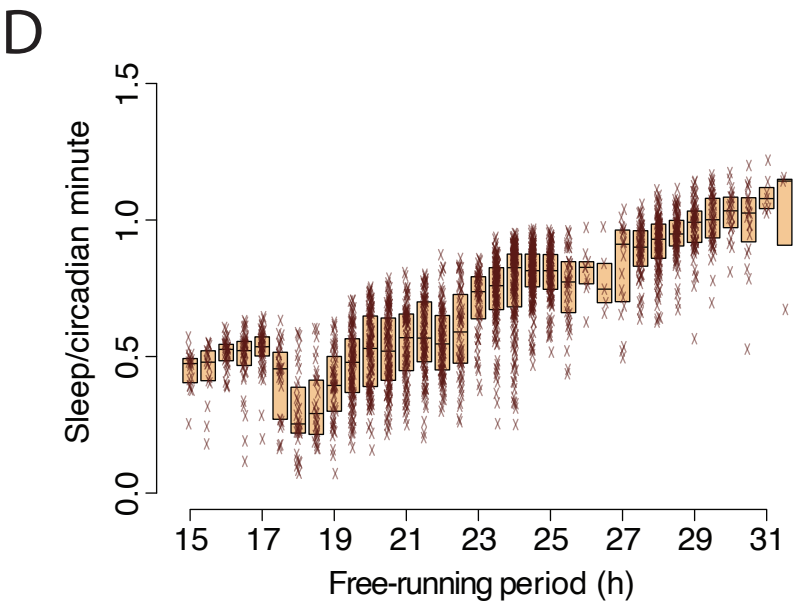
D
Sleep/circadian minute
0.0
0.5
1.0
1.5
15
17
19
21
23
25
27
29
31
Free-running period (h)

Figure 4

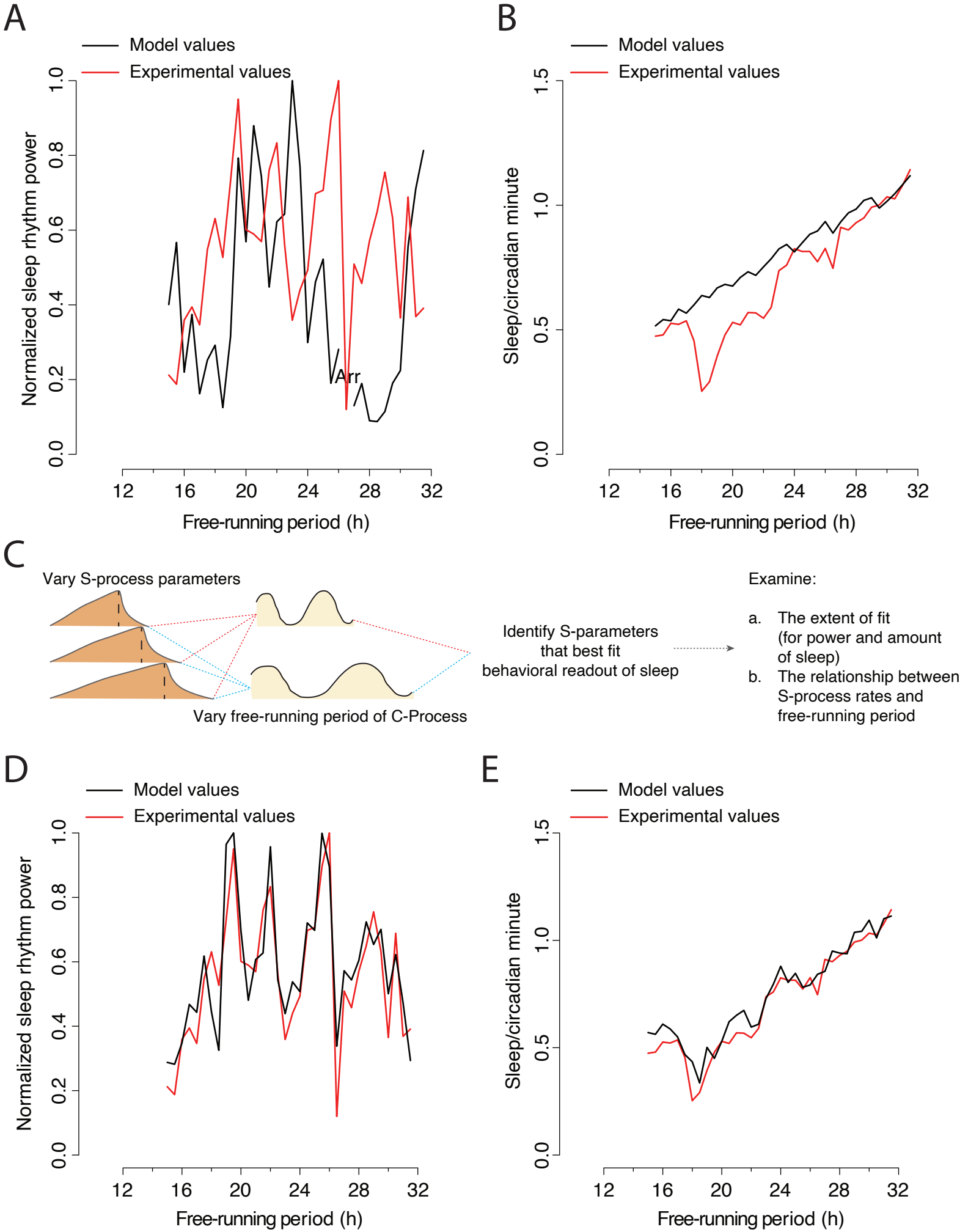
A
Model values
Experimental values
Normalized sleep rhythm power
0.0
0.2
0.4
0.6
0.8
1.0
Arr
12
16
20
24
28
32
Free-running period (h)
B
Model values
Experimental values
Sleep/circadian minute
0.0
0.5
1.0
1.5
12
16
20
24
28
32
Free-running period (h)
C
Vary S-process parameters
Vary free-running period of C-Process
Identify S-parameters
that best fit
behavioral readout of sleep
Examine:
a. The extent of fit
(for power and amount
of sleep)
b. The relationship between
S-process rates and
free-running period
D
Model values
Experimental values
Normalized sleep rhythm power
0.0
0.2
0.4
0.6
0.8
1.0
12
16
20
24
28
32
Free-running period (h)
E
Model values
Experimental values
Sleep/circadian minute
0.0
0.5
1.0
1.5
12
16
20
24
28
32
Free-running period (h)

Figure 5

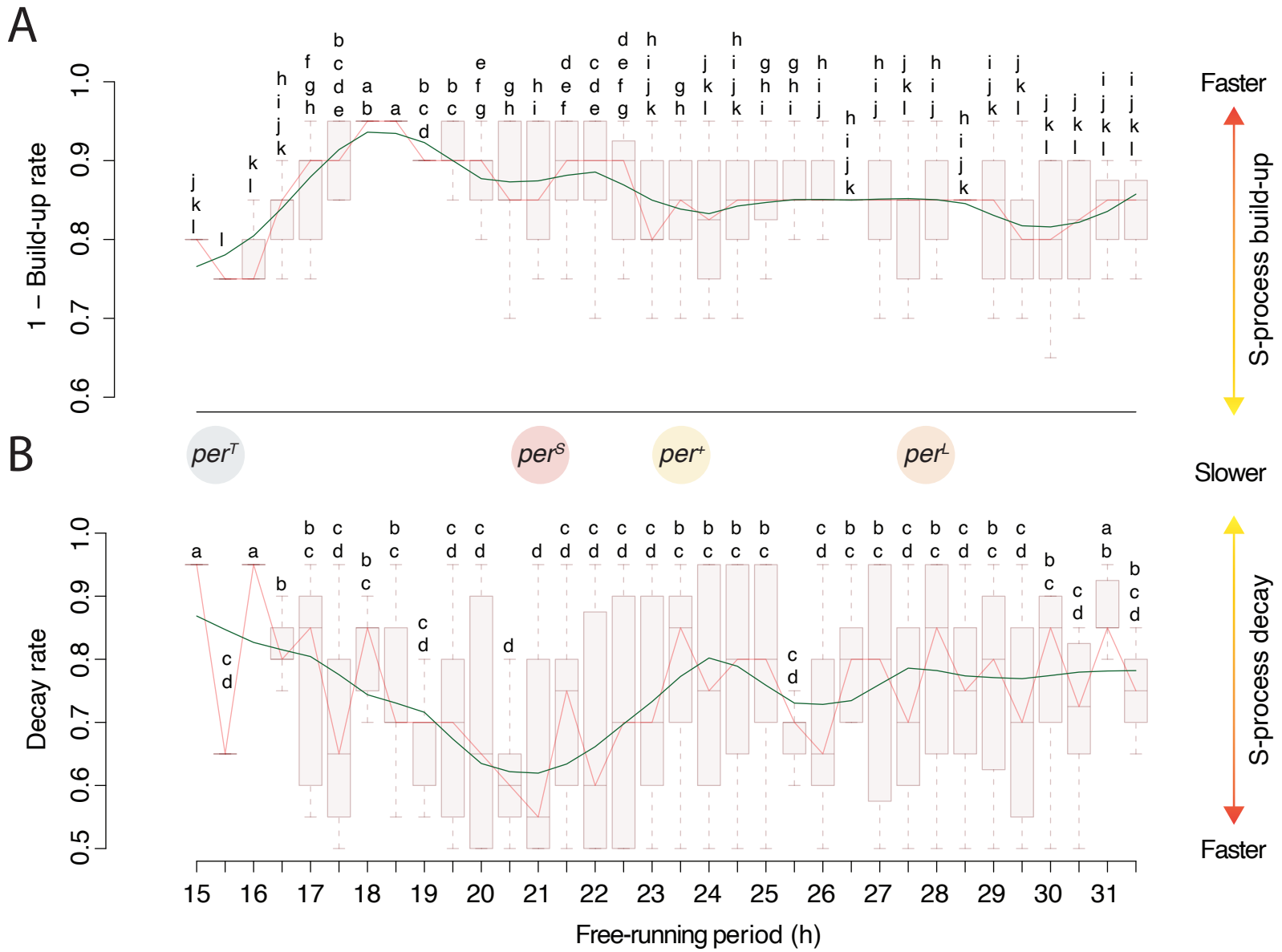
A
1 – Build-up rate
Faster
S-process build-up
B
per^T
per^S
per^+
per^L
Slower
Decay rate
S-process decay
Faster
Free-running period (h)

Figure 6

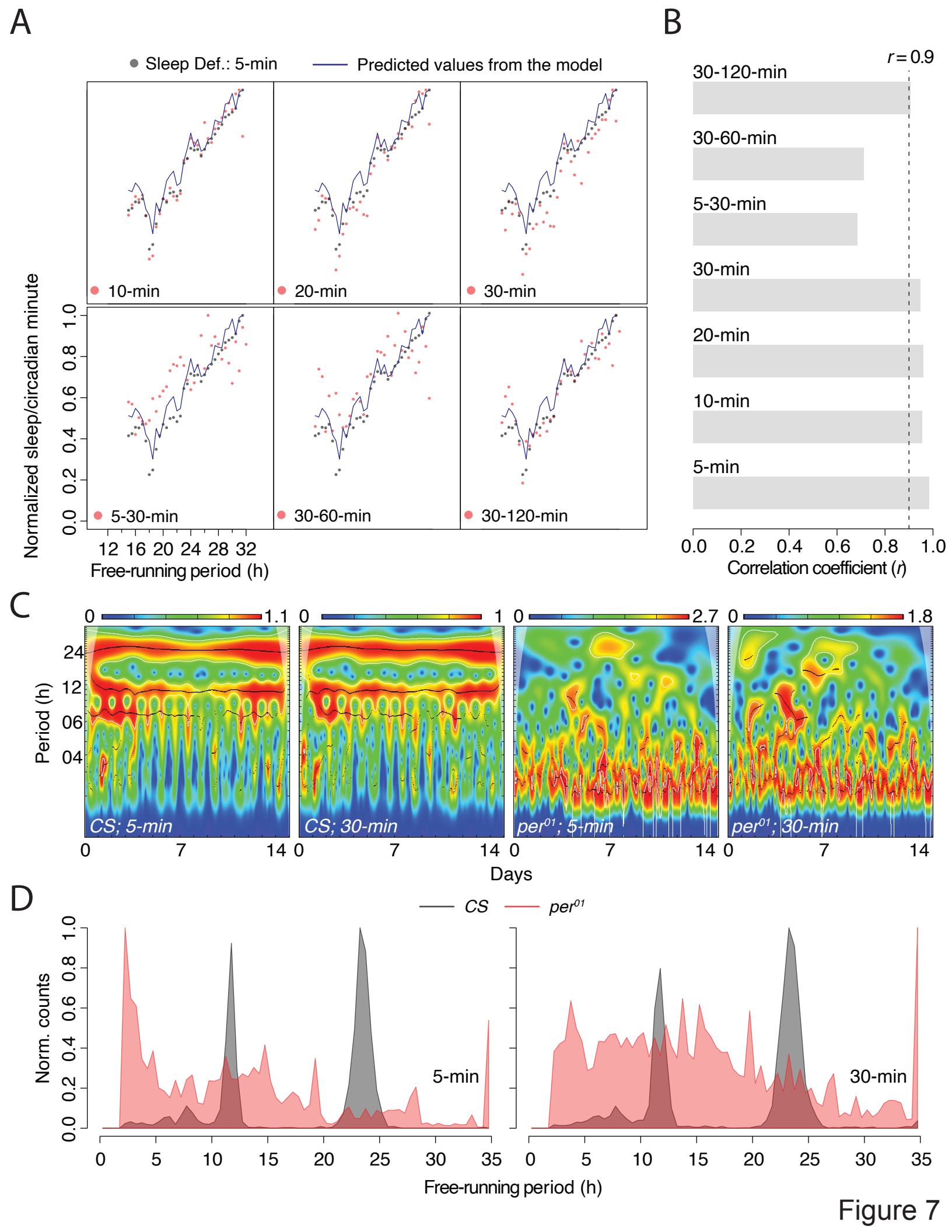
A
Sleep Def.: 5-min
Predicted values from the model
10-min
20-min
30-min
5-30-min
30-60-min
30-120-min
Normalized sleep/circadian minute
0.0
0.2
0.4
0.6
0.8
1.0
12 16 20 24 28 32
Free-running period (h)
B
r = 0.9
30-120-min
30-60-min
5-30-min
30-min
20-min
10-min
5-min
0.0 0.2 0.4 0.6 0.8 1.0
Correlation coefficient (r)
C
0 1.1
0 1
0 2.7
0 1.8
Period (h)
24
12
06
04
CS; 5-min
CS; 30-min
per01; 5-min
per01; 30-min
0 7 14
Days
D
CS
per01
Norm. counts
0.0 0.2 0.4 0.6 0.8 1.0
5-min
30-min
0 5 10 15 20 25 30 35
Free-running period (h)

Figure 7

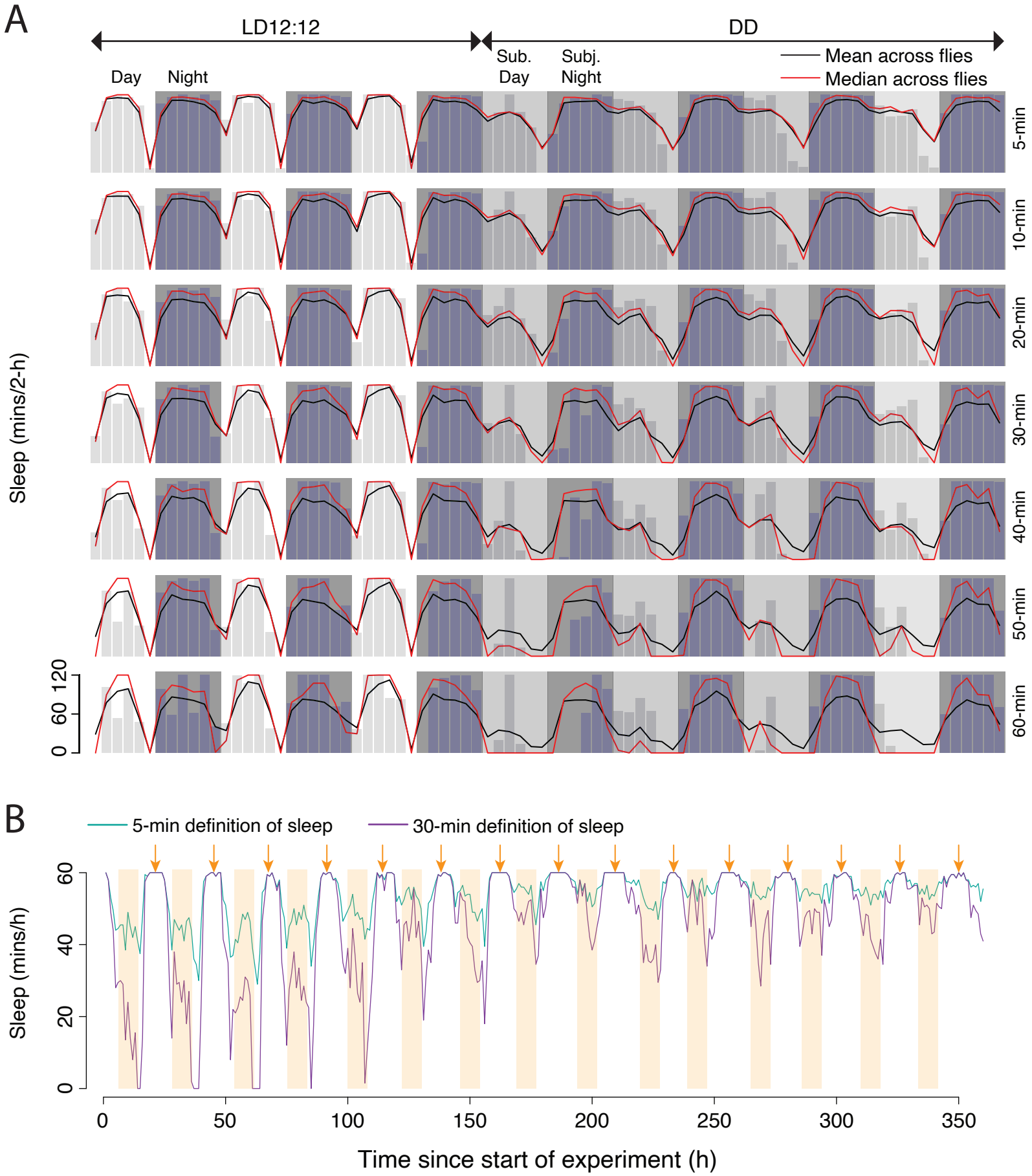
A
LD12:12
DD
Day
Night
Sub. Day
Subj. Night
Mean across flies
Median across flies
5-min
10-min
20-min
30-min
40-min
50-min
60-min
Sleep (mins/2-h)
0
60
120
B
5-min definition of sleep
30-min definition of sleep
Sleep (mins/h)
0
20
40
60
0
50
100
150
200
250
300
350
Time since start of experiment (h)

Figure 8

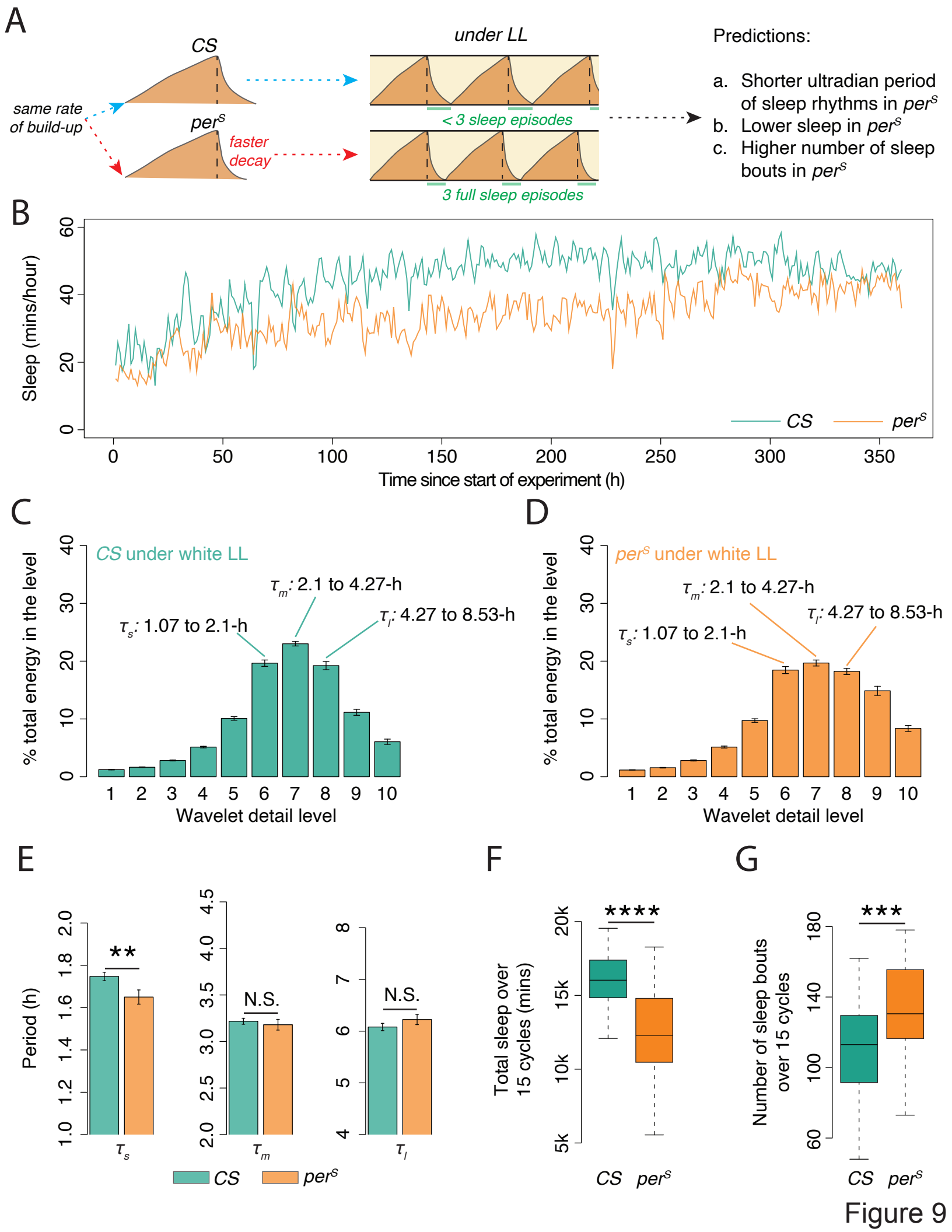
A
CS
per^S
same rate of build-up
faster decay
under LL
< 3 sleep episodes
3 full sleep episodes
Predictions:
a. Shorter ultradian period of sleep rhythms in per^S
b. Lower sleep in per^S
c. Higher number of sleep bouts in per^S
B
Sleep (mins/hour)
Time since start of experiment (h)
CS
per^S
C
CS under white LL
% total energy in the level
Wavelet detail level
τs: 1.07 to 2.1-h
τm: 2.1 to 4.27-h
τl: 4.27 to 8.53-h
D
per^S under white LL
% total energy in the level
Wavelet detail level
τs: 1.07 to 2.1-h
τm: 2.1 to 4.27-h
τl: 4.27 to 8.53-h
E
Period (h)
**
N.S.
N.S.
τs
τm
τl
CS
per^S
F
Total sleep over 15 cycles (mins)
****
CS
per^S
G
Number of sleep bouts over 15 cycles
***
CS
per^S

Figure 9

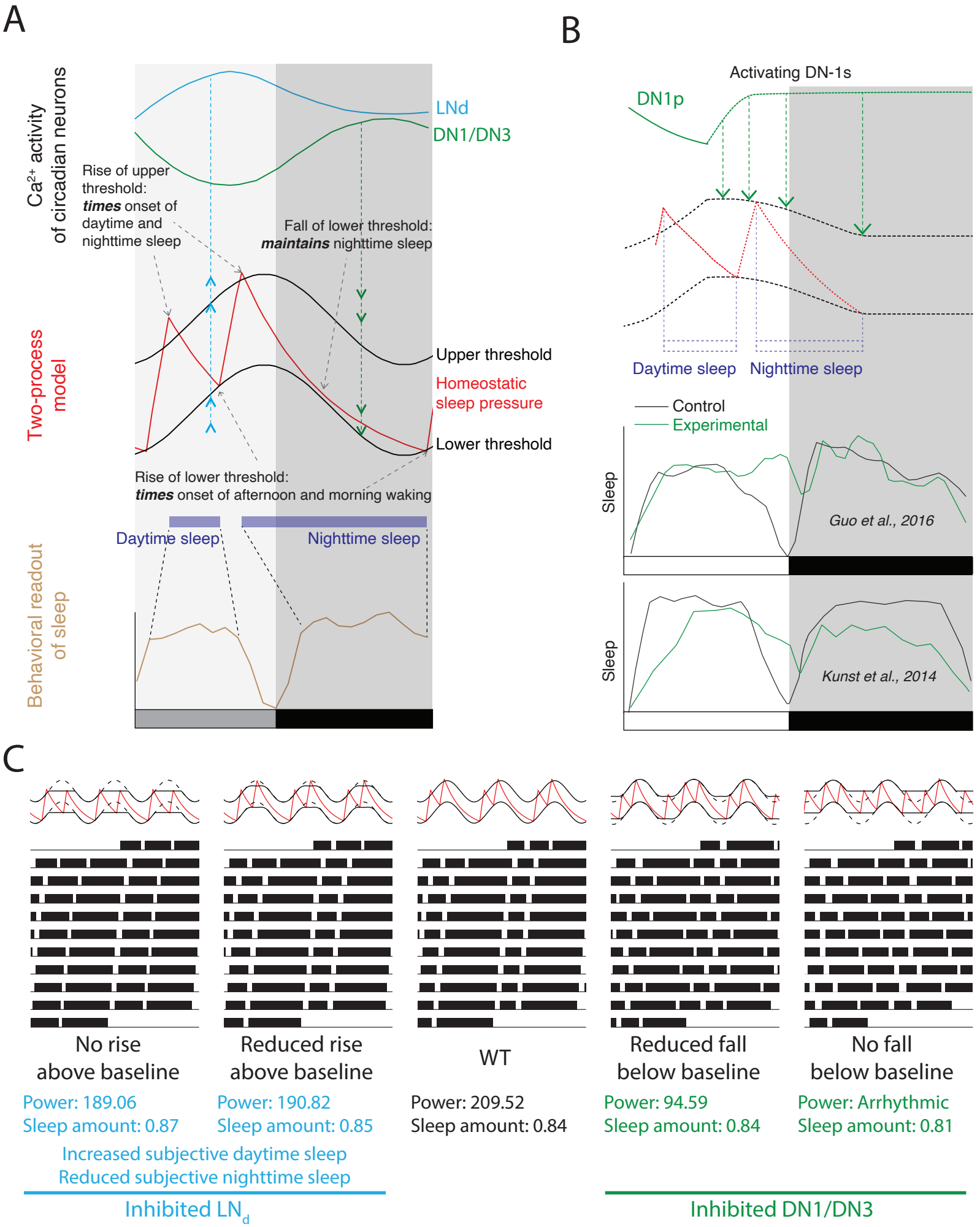
A
Ca2+ activity of circadian neurons
LNd
DN1/DN3
Rise of upper threshold: times onset of daytime and nighttime sleep
Fall of lower threshold: maintains nighttime sleep
Two-process model
Upper threshold
Homeostatic sleep pressure
Lower threshold
Rise of lower threshold: times onset of afternoon and morning waking
Daytime sleep
Nighttime sleep
Behavioral readout of sleep
B
Activating DN-1s
DN1p
Daytime sleep
Nighttime sleep
Control
Experimental
Sleep
Guo et al., 2016
Sleep
Kunst et al., 2014
C
No rise above baseline
Reduced rise above baseline
WT
Reduced fall below baseline
No fall below baseline
Power: 189.06
Sleep amount: 0.87
Power: 190.82
Sleep amount: 0.85
Power: 209.52
Sleep amount: 0.84
Power: 94.59
Sleep amount: 0.84
Power: Arrhythmic
Sleep amount: 0.81
Increased subjective daytime sleep
Reduced subjective nighttime sleep
Inhibited LNd
Inhibited DN1/DN3

Figure 10